Phase Stability of Some Austenitic Stainless Steels at Cryogenic Temperature and under Magnetic Field

(オーステナイト系ステンレス鋼の極低温・磁場下における相安定性)

2009

Jae-hwa Lee
李 載和

Division of Materials and Manufacturing Science
Graduate School of Engineering
Osaka University

Phase Stability of Some Austenitic Stainless Steels at Cryogenic Temperature and under Magnetic Field

(オーステナイト系ステンレス鋼の極低温･磁場下における相安定性)

2009

Jae-hwa Lee
李 哉和

Division of Materials and Manufacturing Science
Graduate School of Engineering
Osaka University

Contents

Chapter 1

Introduction

1. 1 Outline of the present work

Austenitic stainless steels are now extensively used because of their excellent mechanical, chemical and physical properties. These properties include high corrosion resistance, high ductility, high toughness, high workability, excellent weldability and nonmagnetic property[1-6]. Considering these properties, we are confident that, in near future, they will be used more widely under extreme conditions, such as high stress, high magnetic field and low temperature and their combinations, as shown in Fig. 1-1.

Austenitic stainless steels are based on the Fe-Cr-Ni-C system. Nickel stabilizes the austenite phase of steel, maintaining fully austenite phase (γ-phase) at room temperature[7-11], as shown in Fig. 1-2. Chromium improves the corrosion resistance of steel. The austenite

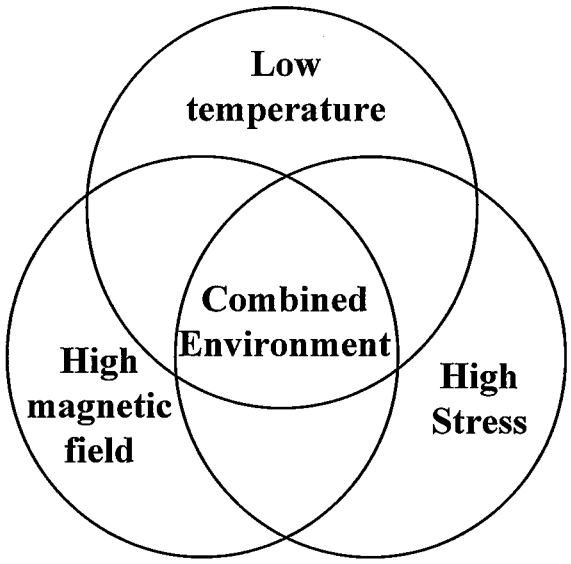

Fig. 1-1 Schematic diagram of extreme conditions, such as high stress, high magnetic field and low temperature and their combinations.

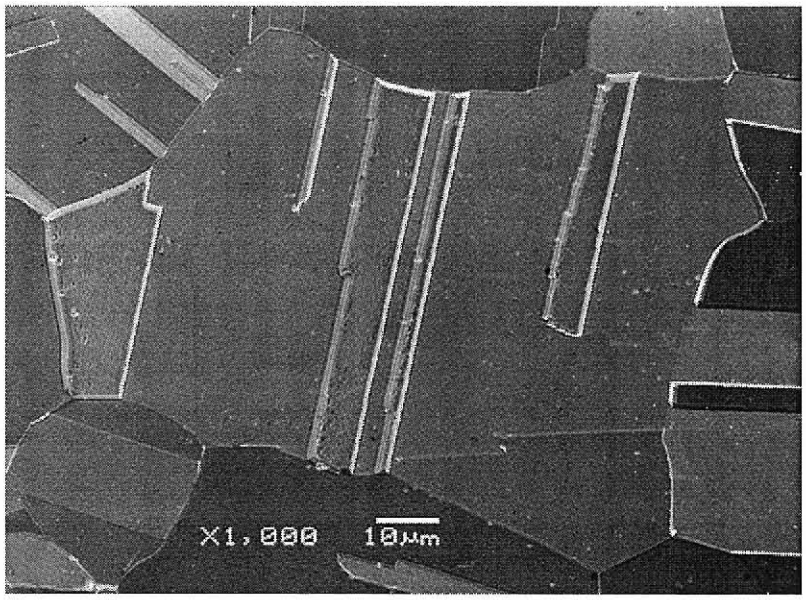

Fig. 1-2 SEM observation result of a fully austenitic phase in solution treated SUS304L austenitic stainless steel.

phase of most stainless steels is, however, metastable, and a martensite phase (ε′-phase and α′-phase) could be induced by applying external fields or by cooling after heat-treatment[12-15]. In most cases, martensitic transformations deteriorate the excellent properties of austenitic stainless steel[16-19]. For example, it can lead to cracks due to the volume change associated with the martensitic transformation. Furthermore, the martensitic transformation accompanies change in magnetic properties[20-23]: the non-magnetic property of austenite phase changes into ferromagnetic one when the α′-phase forms by martensitic transformation. Such a change of magnetic property is not preferable for many applications, especially in which magnetic field is used. Therefore, it is very important to investigate the stability of austenite phase in order to use austenitic stainless steels safely. However, the stability of the austenite phase under extreme conditions described above has not been studied systematically yet. In the present study, therefore, the stability of austenite phase under these extreme conditions has been investigated by using four representative austenitic stainless steels (SUS304, SUS304L, SUS316 and SUS316L). In the following, the background, purpose and construction of the thesis are described.

1. 2 Effect of deformation at low temperature

High stress is one of external fields and influences the phase stability of austenitic stainless steels. Until now, the effects of high stress on martensitic transformation have been studied by many researches[17, 24-28]. Generally, the martensitic transformation is known to be induced in austenitic stainless steels when the steels are deformed at temperatures below M_d.

The γ-phase (fcc) in austenitic stainless steels transforms to α′-martensites (bcc) by deformation. In addition, ε′-martensite (hcp) is also formed as an intermediate phase prior to the formation of α′-martensite in certain austenitic stainless steels. Such a martensitic transformation sequence depends on the chemical composition of stainless steel. (Increasing the amount of Cr addition promotes formation of ε′-martensite.)

Nucleation of deformation-induced α′-martensite in austenitic stainless steels is known to

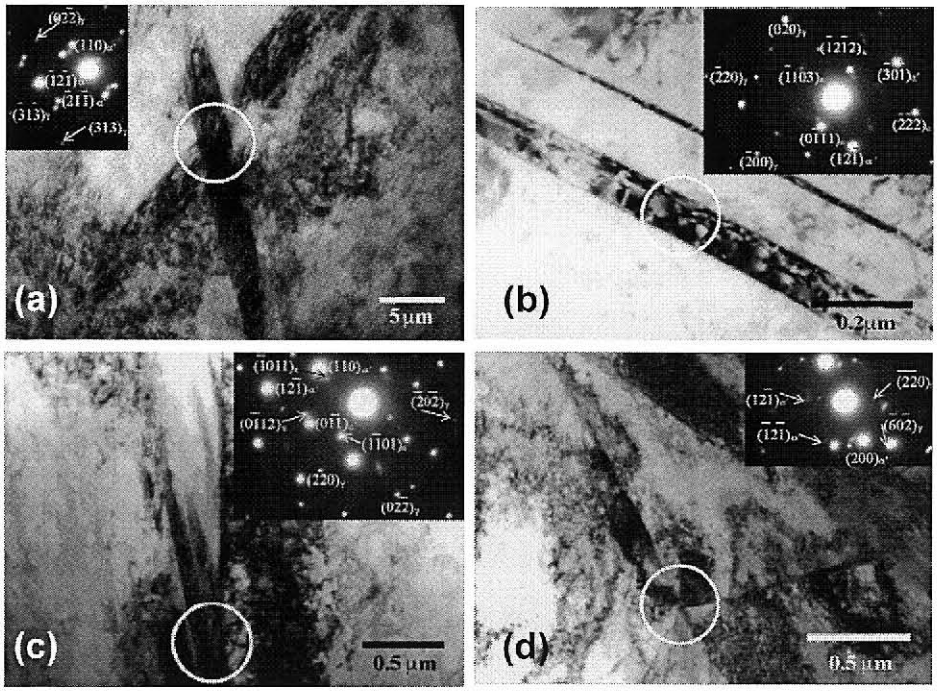

Fig. 1-3 Nucleation sites of α′-martensite in austenite stainless steel: intersection of ε′-martensites (a), isolated ε′-martensite (b), ε′-martensite-grainboundary (c) and grain boundary triple point (d), respectively. (after Das *et at.* [30])

occur at such sites as twins, stacking faults and ε'-martensite. Olson and Cohen assumed that the nucleation of martensite occurs at intersections of above sites[29], as shown in Fig. 1-3 (a), and the rate of martensite formation will therefore be proportional to the rate of shear-band intersection formation. In addition, Das *et al.* reported that the nucleation of the deformation-induced α'-martensite also occurs at isolated shear band, shear band-grain boundary intersection and grain boundary triple point, as shown in Fig. 1-3 (b)-(d)[30].

Huang *et al.*, Guimaraes and Werneck have found that the grain size of the austenitic stainless steel affects the deformation-induced martensitic transformation[31-32]. That is, a decrease in the grain size will generate less deformation-induced martensites. The reason for such grain size dependence is that the grain boundaries suppress the growth of martensites.

The strain rate and the loading condition have been also studied as factors which will influence the deformation-induced martensitic transformation by Peterson *et al.*, Hecker *et al.* and Murr *et al.*[33-35]. The strain rate is believed to have two different effects. First, high strain rates will restricts the amount of deformation-induced martensite. Secondly, the higher strain rate is believed to promote formation of shear-bands, which would promote the strain-induced martensitic transformation due to the formation of more nucleation sites. Patel and Cohen have investigated the effect of the applied stress on the martensitic transformation and found that biaxial stress produces more martensite than uniaxial stress[36].

Although the effect of deformation only is well understand as described above, the combined environment of external stress and magnetic field at cryogenic temperature are not examined yet for austenitic stainless steels.

1. 3 Effect of magnetic field on martensitic transformation

1.3.1 Influence on martensitic transformation temperature

A magnetic field is also one of external fields, and influences martensitic transformation in ferrous alloys and steels, because a large difference in magnetization exists between the

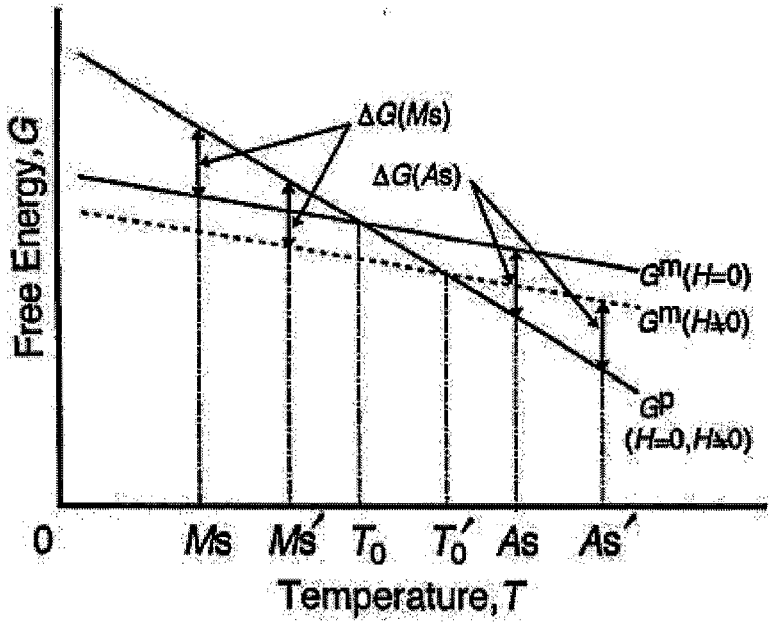

Fig. 1-4 Schematic illustration of Gibbs chemical free energy as a function of temperature in a magnetic field. (after Kakeshita *et al.* [46])

austenitic and martensite phase. We schematically show why the transformation temperature is influenced by the magnetic field. Figure 1-4 schematically shows temperature dependence of the Gibbs chemical free energy of the parent phase (G_p) and the martensite phase (G_m). In the figure, T_0 and M_s represent the equilibrium temperature and transformation start temperature, respectively. When the magnetic field is applied to the system, the Gibbs chemical free energy of the martensite phase decreases mainly due to the addition of the magnetostatic energy (the change in Gibbs chemical free energy of the parent phase is neglected here for simplicity). Therefore, the equilibrium temperature under the magnetic field increases, as shown in Fig. 1-4. Also, the temperature M_s under the magnetic field increases to M_s' if it is assumed that the martensitic transformation under the magnetic field occurs at the temperature where the change between the Gibbs chemical free energies G_p and G_m under the magnetic field is the same as that between the Gibbs chemical free energies under no magnetic field at M_s.

Such effects of magnetic field on martensitic transformation have been studied by many researchers, in particular by Sadovsky *et al.* and by Kakeshita *et al.* As a result, many

interesting phenomena concerning these effects have been discovered[37-42].

1.3.2 Influence on morphology of martensites

Kakeshita *et al.* also researched that the effect of a magnetic field on the morphology and arrangement of martensites[43]. Figure 1-5 shows optical micrographs of thermally-induced martensites formed by cooling a little below the M_s temperature ((a), (d) and (g)) and those of magnetic field-induced martensites ((b), (c), (e), (f), (h) and (i)). The transformation temperature T, ΔT (= T - M_s) and H are shown in each photograph of Fig. 1-5. They reported that, the morphologies of the martensite formed in some steel does not depend on the formation temperature: an Fe-28.7Ni-1.8C alloy (mass %) exhibits thin plate morphology and the other two alloys a lenticular one in all cases. They also pointed out that the morphologies of martensites are different even if the martensites are formed at nearly the same temperature, as

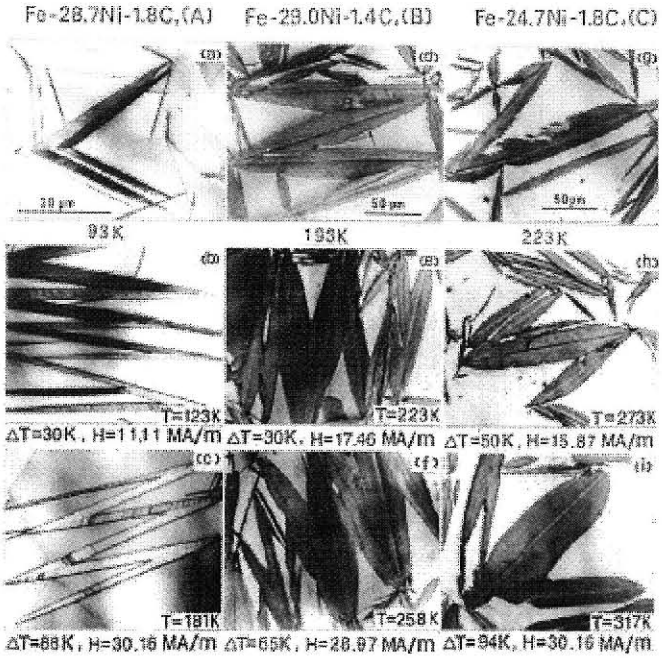

Fig. 1-5 Optical micrographs of thermally-induced martensites, (a) and (d), and magnetic field-induced ones, (b), (c), (e) and (f). Transformation temperature T, ΔT and H for the magnetic field-induced martensites are shown in each photograph. (after Kakeshita *et al.* [44])

seen from the comparison of (c) and (d). This result is contradictory to a proposition that the martensite morphology in Fe-Ni-C alloys is decided only by the formation temperature. The reason for this difference is not known yet. The same results (the morphology of a magnetic field-induced martensite was the same as that of a thermally induced one irrespective of the transformation temperature and the strength of the magnetic field) are obtained for Fe-Ni[44] and Fe-Mn-C[45] alloys.

1.3.3 Kinetics of martensitic transformation

Martensitic transformations are classified into two groups from the view point of kinetics: athermal and isothermal ones by a difference in time and temperature dependence of the amount of martensites. The amount of the athermal martensite has been considered to be a function of temperature only. The athermal martensitic transformation has been considered not to take place until the temperature is brought down below M_s, the martensitic transformation start

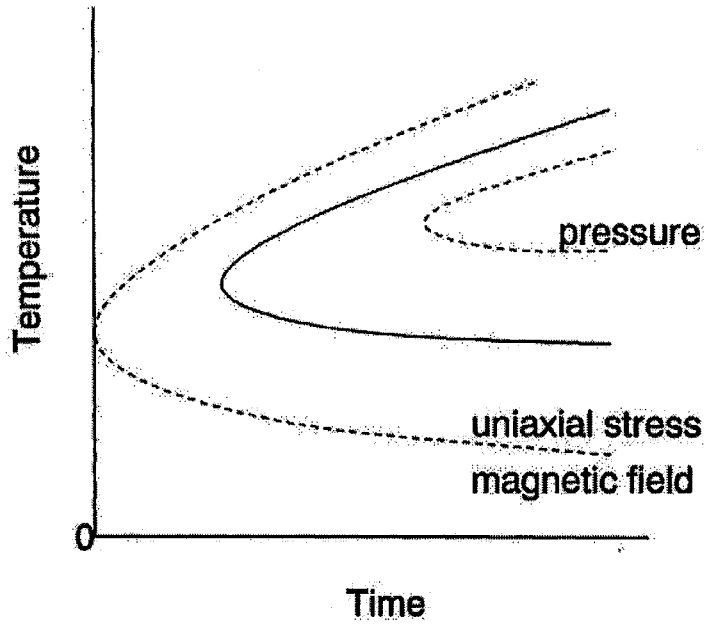

Fig. 1-6 Predicted *TTT* diagrams of isothermal martensitic transformation under magnetic field and hydrostatic pressure by the theory previously constructed, together with that under no external filed. (after Kakeshita *et al.* [47])

temperature, which is always below the thermodynamical equilibrium temperature, T_0, between the parent and martensite phases. On the other hand, the amount of isothermal martensite has been thought to be dependent on both temperature and time, where a waiting time or an incubation time is needed until the martensite transformation starts while the temperature is kept constant. Materials undergoing such an isothermal martensitic transformation are very few in number, and an Fe-Ni-Mn alloy is a typical example. However, there is a view that the isothermal transformation is general and the athermal one is unique, speculating that the incubation time needed for the athermal transformation is undetectably short. Unfortunately, this view has not been verified yet, although the verification may give important information on the basic problems, such as thermodynamics, nucleation and growth mechanism and the origin of martensitic transformation.

Recently, Kakeshita *et al.* have found that the originally isothermal kinetics of martensitic transformation in Fe-Ni-Mn based alloy changed to an athermal one under pulsed magnetic field, and they have also performed a systematic study on the incubation time in Fe-Ni-Mn alloys under magnetic field[46-47]. They have explained their experimental results by introducing a phenomenological theory. Their theory is based on the probability related to the nucleation barrier. Moreover, it is predicted that the athermal martensitic transformation can be explained by the same kinetics as the isothermal martensitic transformation. Details of the theory is reported elsewhere[48].

Based on the theory, they made the following predictions about the behavior of athermal and isothermal martensitic transformations, as schematically shown in Fig. 1-6[47]: (i) a static magnetic field lowers the nose temperature and shortens the incubation time; (ii) a hydrostatic pressure raises the nose temperature and increases the incubation time; (iii) in materials classified as exhibiting an athermal transformation, the transformation occurs isothermally by holding at a temperature between T_0 and M_s.

Similar effects of magnetic field are also expected to occur in austenitic stainless steel because α′-martensite in stainless steels is ferromagnetic. However, there is almost no report concerning such effects in austenitic stainless steel.

1.4 Effect of heat-treatment

In many application of stainless steels, a welding process is unavoidable and during the welding process, the steels induce carbide precipitation ($M_{23}C_6$) along the grain boundaries[49], as illustrated in Fig. 1-7. The precipitation of $M_{23}C_6$ is preceded by intermediate phases in the sequence of cementite, M_2X and M_7C_3, and finally leading to $M_{23}C_6$[50]. Characteristics of $M_{23}C_6$ precipitates are usually investigated by sensitization heat-treatment; the stainless steels are heat-treated in the temperature range between 773 and 1073 K. Such a carbide precipitation along the grain boundaries forms the chromium depleted zone, which enfeebles the formation of passive film and leads to preferential corrosion[5, 51-52].

The formation of carbide precipitation of $M_{23}C_6$ is also known to induce α'-martensite in some austenitic stainless steels[14, 17]. This formation of ferromagnetic α'-martensite is attributed to decrease in nickel and chromium concentrations, which are important elements to maintain the austenite phase at room temperature, as mentioned above. Such a formation of

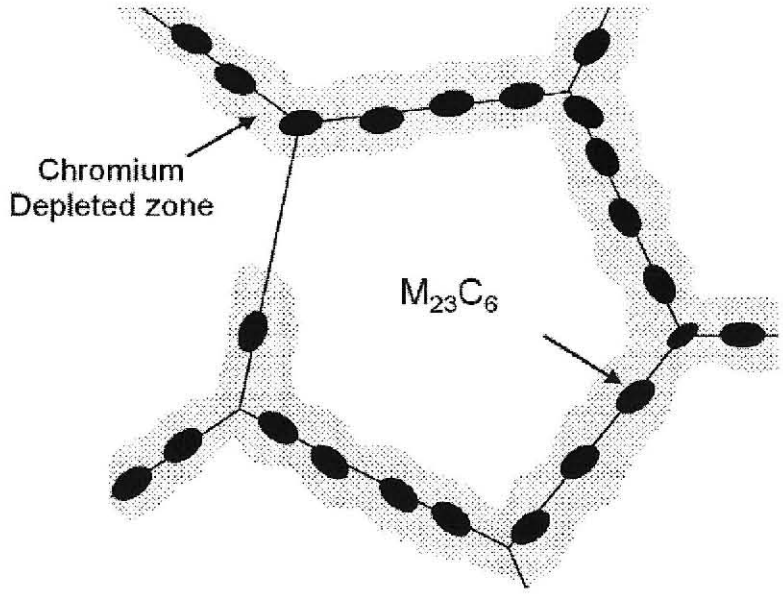

Fig. 1-7 Schematic diagram of carbide precipitation formed along the grain boundaries.

α′-martensite alters non-magnetic property in some austenitic stainless steels to ferromagnetic one after sensitization heat-treatment.

1.5 Purpose and Construction

As mentioned above, austenitic stainless steels will be used under the extreme environments, such as cryogenic temperature, high stress, high magnetic field and their combined environments because of their excellent properties. Such extreme environments (external fields) could influence the phase stability of austenitic stainless steels as described above. Therefore, it is important to clarify the effects of the external fields on martensitic transformation for using the austenitic stainless steels safely and for obtaining the information on the basic problems, such as kinetics and crystallography of martensitic transformation in austenitic stainless steels. In addition, it is also reported that the sensitization heat-treatment influence on the phase stability of austenitic stainless steel by many previous researches[14, 17]. Therefore, investigation, the effect of the sensitization heat-treatment on the stability of austenite phase, is also necessary. However, there have been not so much such studies.

In the present study, therefore, we will investigate the effects of cryogenic temperature, high magnetic field, high stress and their combined conditions on martensitic transformation in the solution-treated and sensitized typical austenitic stainless steels (SUS304, SUS304L, SUS316 and SUS316L).

The thesis consists of the following six chapters:

Chapter 1 The background of the present study was introduced and the purpose and significance of the present study were described.

Chapter 2 The effects of cryogenic temperature, high magnetic field, high stress and their combined conditions on martensitic transformation in solution-treated and sensitized SUS304, SUS304L, SUS316 and SUS316L stainless steels are described.

Chapter 3 Time-temperature-transformation diagram of isothermal martensitic transformation in a solution-treated SUS304L stainless steel is described.

Chapter 4 Time-temperature-transformation diagram of isothermal martensitic transformation in a sensitized SUS304 stainless steel is described.

Chapter 5 The effect of magnetic field on successive $\gamma \rightarrow \varepsilon' \rightarrow \alpha'$ martensitic transformation in a solution-treated SUS304L stainless steel is described.

Chapter 6 The results obtained in this study are summarized.

References

[1] S. Murase, S. Kobatake, M. Tanaka, I. Tashiro, O. Horigami, H. Ogiwara, K. Shibata, K. Nagai and K. Ishikawa, *Fusion Eng. Des.* **20** (1993) 451

[2] J. W. Chan, D. Chu, A. J. Sunwoo and J. W. Morris, Jr., *Cryogenic Engineering (Materials)* **38** (1992) 55

[3] D. C. Larbalestier and H.W. King, *Cryogenics* **13** (1973) 160

[4] D. T. Read and R. P. Reed, *Cryogenics* **21** (1981) 415

[5] T. Tanaka, T. Kadota, Y. Kohno and K. Shibata, *Advances in Cryogenic Engineering and Materials* **44** (1998) 1

[6] N. Yasumaru, *Mater. Trans.* **39** (1998) 1046

[7] S. K. Varma, J. Kalyanam, L. E. Murr and V. Srinivas, *J. Mater. Sci. Lett.* **13** (1994) 107

[8] V. Shrinivas, S. K. Varma and L. E. Murr, *Metall. Mater. Trans. A* **26A** (1995) 661

[9] J. Sort and A. Concustell, E. Menendez, S. Surinach, M.D. Baro, J. Farran and J. Nogues, *J. Appl. Phys. Lett.* **89** (2006) 032509

[10] A. Szyman´ska, D. Oleszak, A. Grabias, M. Rosinski, K. Sikorski, J. Kazior, A. Michalski and K. J. Kurzydlowski, *Rev. Adv. Mater. Sci.* **8** (2004) 143

[11] F. Lecroisey and A. Pineau, *Metal. Trans.* **3** (1972) 387

[12] H. C. Shin, T. K. Ha and Y. W. Chang, *Scripta Mater.* **45** (2001) 823

[13] Pat L. Mangonon Jr., G. Thomas, *Metall. Trans.* **1** (1970) 1577

[14] S. Takaya, T. Suzuki, Y. Matsumoto, K. Demachi, M. Usesaka, *J. Nucl. Mater.* **327** (2004) 19

[15] S. S. Hecker, M. G. Stout, K. P. Staudhammer and J. L. Smith, *Metall. Trans. A* **13A** (1982) 619

[16] E. Nagy, V. Mertinger, F. Tranta and J. Sólyom, *Mater. Sci. Eng. A* **378** (2004) 308

[17] K. Mumtaz, S. Takahashi, J. Echigoya, L. F. Zhang, Y. Kamada and M. Sato, *J. Mater. Sci.* **38** (2003) 3037

[18] K. Mumtaz, S. Takahashi, J. Echigoya, Y. Kamada, L. F. Zhang, H. Kikuchi, K. Ara and M.

Sato, *J. Mater. Sci.* **39** (2004) 1997

[19] L. Zhang, S. Takahashi, Y. Kamada, H. Kikuchi, K. Ara, M. Sato and T. Tsukada, *J. Mater. Sci.* **40** (2005) 2709

[20] Y. Kamada, T. Mikami, S. Takahashi, H. Kikuchi, S. Kobayashi and K. Ara, *J. Magn. Magn. Mater.* **310** (2007) 2856

[21] A. Miller, Y. Estrin and X. Z. Hu, *Scripta Mater* **47** (2002) 441

[22] A. Mitra, P. K. Srivastava, P. K. De, D. K. Bhattacharya and D. C. Jiles, *Metall. Mater. Trans. A* **35A** (2004) 559

[23] F. De Backer, V. Schoss and G. Maussner, *Nucl. Eng. Des.* **206** (2001) 201

[24] L. Zhao, N.H. van Dijk, E. Bruck, J. Sietsma and S. van der Zwaag, *Mater. Sci. Eng. A* **313** (2001) 145

[25] G. B. Olson and M. Cohen, *J. Less-Common Met.* **28** (1972) 107

[26] F. Lecroisey and A. Pineau, *Metall. Trans.* **3** (1972) 387

[27] L. Mangonon Jr. and G. Thomas, *Metall. Trans.* **1A** (1970) 1577

[28] T. Suzuki, H. Kojima, K. Suzuki, T. Hashimoto and M. Ichihara, *Acta Metall.* **25** (1977) 1151

[29] G. B. Olson and M. Cohen, *Metall. Trans.* **6A** (1975) 791

[30] A. Das, S. Sivaprasad, M. Ghosh, P. C. Chakraborti, S. Tarafder, *Mater. Sci. Eng. A* **486** (2008) 283

[31] C. Guimaraes and V. P. Werneck, *Marls. Sci. and Eng.* **34** (1978) 87

[32] G. L. Huang, D. K. Matlock and G. Krauss, *Metall. Trans. A* **20** (1989) 1239

[33] S. F. Peterson, M. C. Mataya and D. K. Matlock, *JOM* **49** (1997) 54

[34] L. E. Murr, K. P. Staudhammer and S. S. Hecker, *Metall. Trans. A* **13A** (1982) 627

[35] S. S. Hecker, M. G. Stout, K. P. Staudhammer and J. L. Smith, *Metall. Trans. A* **13A** (1982) 627

[36] J. R. Patel and M. Cohen, *Acta Metall.* **1** (1953) 532

[37] V. D. Sadovsky, N. M. Rodigin, L. V. Smirnov, G. M. Filonchik and I. G. Fakidov, *Fiz. Met. Metalloved* **12** (1961) 302

[38] P. A. Malinen and V. D. Sadovsky, *Fiz. Met. Metalloved* **28** (1969) 1012

[39] Y. A. Fokina, L. V. Smirnov, V. D. Sadovsky and A. F. Prekul, *Fiz. Met. Metalloved* **19** (1965) 932

[40] T. Kakeshita, K. Shimizu, S. Funada and M. Date, *Trans. Jap. Inst. Met. 25* (1984) 837

[41] T. Kakeshita, H. Shirai, K. Shimizu, K. Sugiyama, K. Hazumi and M. Date, *Trans. Jpn. Inst. Met* **29** (1988) 553

[42] T. Kakeshita, T. Saburi, K. Kindo and S. Endo, *Phase Transitions* **70** (1999) 65

[43] T. Kakeshita, K. Shimizu, S. Kijima, T. Yu and M. Date, *Trans. JIM* **26** (1985) 630

[44] T. Kakeshita, K. Shimizu, S. Funada and M. Date, *Acta Metall.* **33** (1985) 1381

[45] T. Kakeshita, H. Shirai, K. Shimizu, K. Sugiyama, K. Hazumi and M. Date, *Trans. JIM* **28** (1987) 891

[46] T. Kakeshita, T. Saburi and K. Shimizu, *Mater. Sci. Eng. A* **273-275** (1999) 21

[47] T. Kakeshita, K. Kuroiwa, K. Shimizu, T. Ikeda, A. Yamagishi and M. Date, *Trans. JIM* **34** (1993) 423

[48] T. Kakeshita, T. Yamamoto, K. Shimizu, K. Sugiyama and S. Endo, *Trans. JIM* **36** (1995) 1018

[49] S.M. Bruemmer and L.A. Charlot, *Scr. Metall.* **20** (1986) 1019

[50] R. G. Baker and J. Nuiting, *J. Iron Steel Inst.* **192** (1959) 257

[51] N. Parvathavarthini and R.K. Dayal, *J. of Nuclear Materials* **305** (2002) 209

[52] V. Kain, R.C. Prasad and P.K. De, *Corrosion* **58** (2002) 15

Chapter 2

Effects of cryogenic temperature, high stress and high magnetic field on phase stability of some austenitic stainless steels

2.1 Introduction

Austenitic stainless steels are widely used because of their desirable feature such as high corrosion resistance, excellent formability, superior weldability, nonmagnetic characteristics and high toughness[1-6]. Considering recent developments in high magnetic field technologies, we are confident that austenitic stainless steels will be used more widely under a combined environment of cryogenic temperature, high stress and high magnetic field in near future. However, the austenite phase in stainless steels tends to become unstable under a cryogenic temperature, high stress and high magnetic field[7-12]. Thus these effects should be well understood in order to use the austenitic stainless steel safely under such combined environment. Concerning the instability of the austenite phase, a martensitic $\gamma \rightarrow \varepsilon' \rightarrow \alpha'$ transformation has been reported to occur in some austenitic stainless steels. The effect of the combined environment described above on the martensitic transformation is especially important because many of the excellent properties could be deteriorated if the austenite phase transforms to the martensite phase[3, 13-16]. There are several investigations concerning the effect of moderate magnetic field on deformation. For example, flow-stress of deformation is reported to increase under a magnetic field of 14 MA/m at cryogenic temperature in some steels because of an enhanced martensitic $\gamma \rightarrow \alpha'$ transformation[17], while no effect of magnetic field (3 MA/m) on martensitic transformation was detected in other report[18]. Change in deformation stress under the magnetic field was also reported in some austenitic stainless steels[19-20]. However, there are few investigations concerning effects of high magnetic field on the stability of the

austenite phase. Therefore, in the present study, we will examine the effects of cryogenic temperature, high stress and high magnetic field and their combined environment on the phase stability of typical austenitic stainless steels of SUS304, SUS304L, SUS316 and SUS316L.

2.2 Experimental Procedure

In the present study, four kinds of austenitic stainless steels, SUS304, SUS304L, SUS316 and SUS304L, were examined. The chemical compositions of the steels are shown in Table 2-1. All kinds of steels were cold-rolled into a sheet. Specimens for various experiments were cut from the sheets to a suitable size, and then solution-treated at 1323 K for 0.5 h followed by quenching into iced water. Some of the specimens were sensitized by heat-treatment at 973 K for 10 or 100 h. The oxidized surface layer was eliminated by electropolishing, where an electrolyte composed of 85 % C_2H_5OH and 15 % $HClO_4$ in volume was used.

The phase stability of stainless steels at cryogenic temperature was examined by two methods: one was magnetic susceptibility measurement at temperatures between 4.2 and 300 K with a constant rate of 1 K/min, and the other was magnetization measurement after isothermal holding at 77 K. Effect of high magnetic field on transformation behavior was examined by using a pulsed magnet with a maximum magnetic field of 30 MA/m. Since it is well known that a deformation at cryogenic temperature for the present steels induces martensite phase[5-6, 21-23], we carried out the tensile test on the present steels at 77 K using an Instron-type tensile machine with a constant strain rate of $2.6 \times 10^{-4}\ s^{-1}$. In order to examine the effect of combined environment on transformation behavior, we applied a magnetic field at 77 or 4.2 K on a specimen which was deformed beforehand at 77 K. The amount of α' martensite formed by the above environment was obtained by a magnetization measurement in a low field range at room temperature. The microstructure and crystal structure of the specimens were investigated by optical microscopy, scanning electron microscopy (SEM) and transmission electron microscopy (TEM). Specimens for TEM observation were prepared by electropolishing using

an electrolyte consisting of 90 % CH_3COOH and 10 % $HClO_4$ in volume. TEM observation was made with an accelerating voltage of 200 kV.

Table 2-1 Composition of austenitic stainless steels used (mass %)

Type	C	Si	Mn	P	S	Ni	Cr	Mo	Fe
SUS304	0.06	0.67	1.01	0.029	0.009	8.50	18.10	–	Bal.
SUS304L	0.023	0.48	1.07	–	0.005	8.47	18.20	–	Bal.
SUS316	0.052	0.67	1.49	0.033	0.005	10.71	16.43	2.12	Bal.
SUS316L	0.015	0.56	0.86	–	0.001	12.36	17.21	2.31	Bal.

2.3 Results

2.3.1 Effect of cryogenic temperature on transformation behavior

In order to investigate the martensitic transformation behavior and magnetic properties, we have measured temperature dependence of magnetic susceptibility by applying a low magnetic field of 79.6 kA/m. Figure 2-1 (a) shows temperature dependence of magnetic susceptibility χ of the SUS304 stainless steel in the solution-treated and sensitized states. The χ-T curve of the solution-treated SUS304 stainless steel shows a sharp peak at about 40 K due to a paramagnetic to antiferromagnetic transition of the γ-phase, being in agreement with a previous report by U. Gonser *et al*[24]. There is no hysteresis between heating and cooling processes. On the other hand, the χ-T curve of the SUS304 stainless steel sensitized for 10 h starts to increase in the cooling process near 260 K due to the formation of ferromagnetic α′-phase. It also starts to increase near 120 K in the heating process. This behavior means that the martensitic transformation of the sensitized SUS304 stainless steel proceeds isothermally. Figure 2-1 (b) shows the χ-T curves of the solution-treated and sensitized SUS304L stainless steel. These results of the both specimens exhibit an increase in susceptibility in the cooling and heating processes between about 160 and 80 K due to the isothermal martensitic transformation as in the

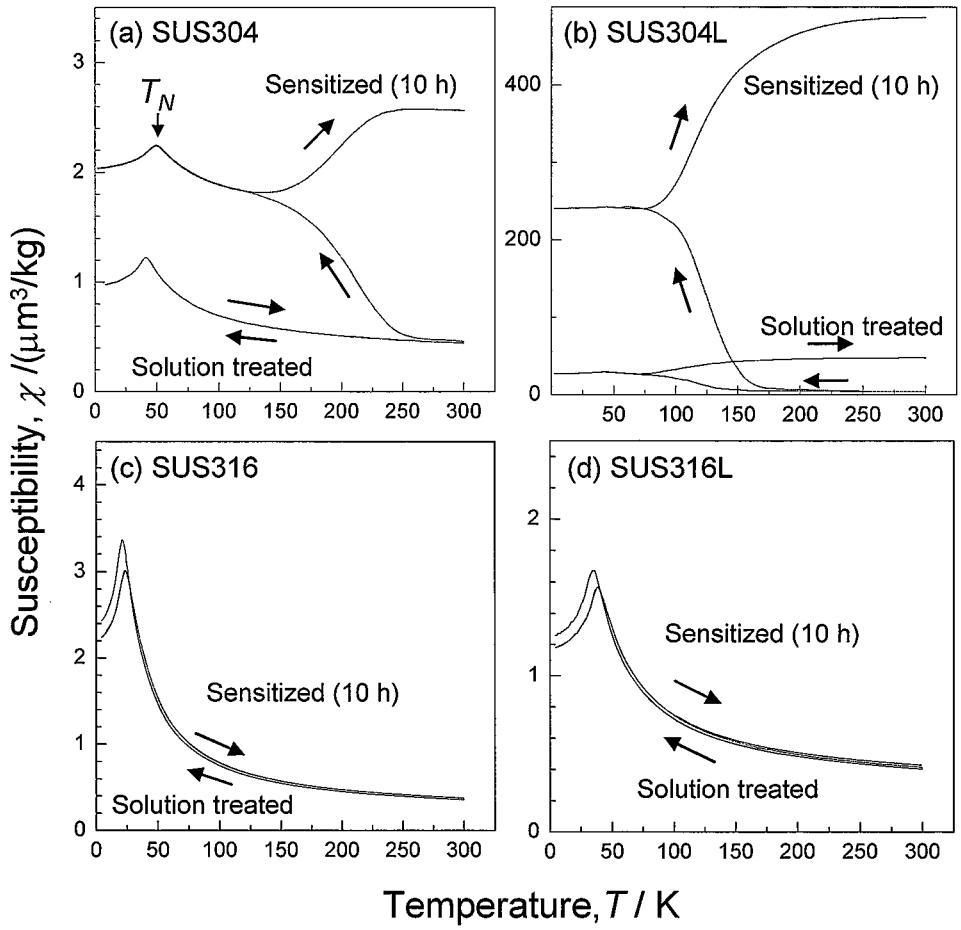

Fig. 2-1 (a-d) Magnetic susceptibility of solution-treated and sensitized stainless steels. Measurement was made in the cooling process and then in the heating process.

sensitized SUS304 stainless steel. However, the isothermal martensitic transformation was not detected in SUS316 and SUS316L stainless steels regardless of heat-treatment, as shown in Fig. 2-1 (c and d). For all steels examined, the Néel temperatures (T_N) slightly increases by sensitization treatment possibly due to the decrease in Cr content of the γ-phase associated with the precipitation of $M_{23}C_6$. We confirmed that an athermal martensitic transformation does not occur for all the steels examined regardless of heat-treatment when the specimen is cooled rapidly. In order to clarify the isothermal martensitic transformation behavior, we have carried out isothermal holding experiment. Figures 2-2 (a) and (b) show the magnetization curves obtained at room temperature, T_R, for a solution-treated SUS304L stainless steel without and

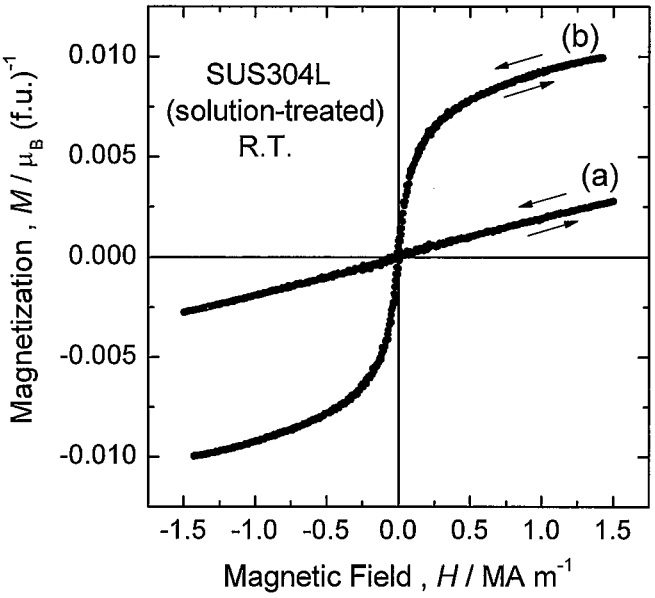

Fig. 2-2 Magnetization curves at R.T. for a solution-treated SUS304L stainless steel; (a) is the specimen without isothermal holding at 77 K and (b) is the specimen after isothermal holding at 77 K for 10^6 s.

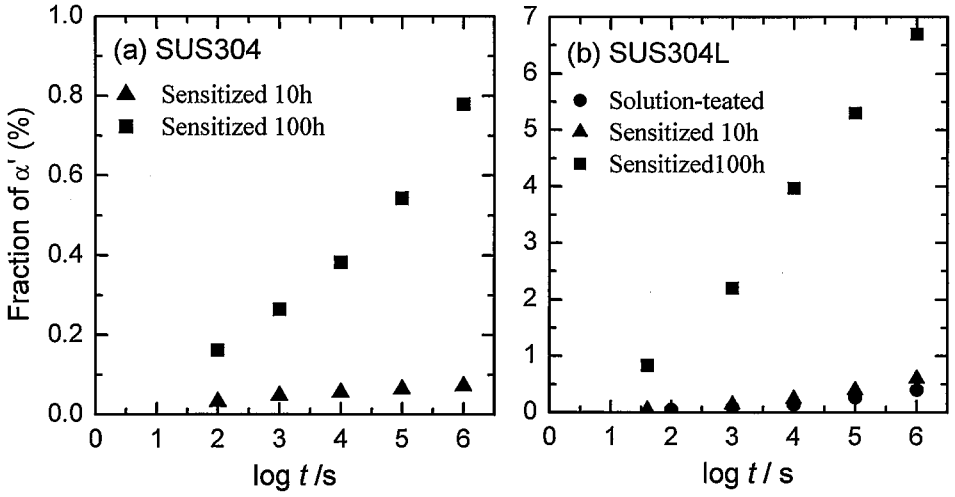

Fig. 2-3 Fraction of the α′-phase formed by isothermal holding at 77 K in the sensitized SUS304, the solution treated and sensitized SUS304L stainless steels.

with isothermal holding at 77 K for 10^6 s, respectively. As known from the figure, the spontaneous magnetization does not appear in the specimen without isothermal holing, while it appears in the specimen with isothermal holding. Similar magnetization measurements were

made for the solution-treated SUS304, sensitized SUS304 and SUS304L stainless steels with different time of isothermal holding. Then, the relation between isothermal holding time at 77 K and the amount of α′ martensite, $f_{\alpha'}$, is shown in Fig. 2-3. The value of $f_{\alpha'}$ was calculated from the spontaneous magnetization of the specimen at room temperature $M_0(T_R)$, and that of the α′ phase $M_0^{\alpha'}(T_R)$ as $f_{\alpha'} = M_0(T_R) / M_0^{\alpha'}(T_R)$. Here, the magnetization of γ- and ε′-phase are neglected because they are nonmagnetic[25-28]. The value of $M_0^{\alpha'}(T_R)$ is approximated as the value at 0 K, $M_0^{\alpha'}(0)$ because the Currie temperature is far above T_R, although it is a rough approximation. The value of $M_0^{\alpha'}(0)$ for SUS304 and SUS304L stainless steels is estimated to be 1.79 μ_B/atom considering the Slater-Pauling curve and their valence electron concentration[29]. We know from Fig. 2-3 that $f_{\alpha'}$ increases with increasing holding time, and also increases with increasing sensitization time for both steels. In the case of the sensitized SUS304L stainless steel, $f_{\alpha'}$ is about one order in magnitude larger than that in the sensitized SUS304 stainless steel.

In order to know isothermal transformation sequence in the present steels, we have made SEM and TEM observations. Figure 2-4 shows a SEM observation result of a solution-treated

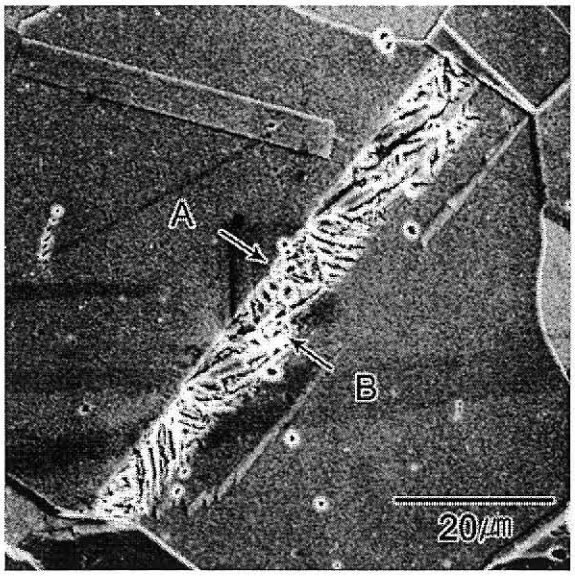

Fig. 2-4 A SEM image of a solution-treated SUS304L stainless steel after isothermal holding at 77 K for 10^6 s. The mark 'A' indicates a plate of ε′-martensite and the mark 'B' indicates a wedge-shaped plate of α′-martensite inside the ε′-martensite.

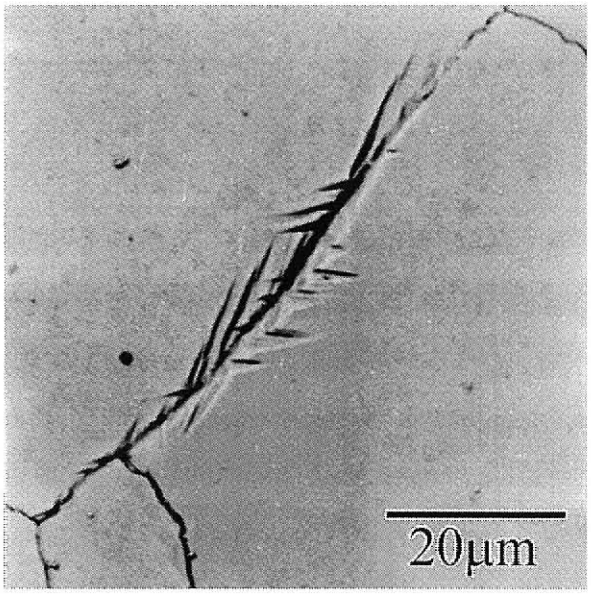

Fig. 2-5 An optical micrograph of a sensitized SUS304 stainless steel after isothermal holding at 77 K for 10^6 s.

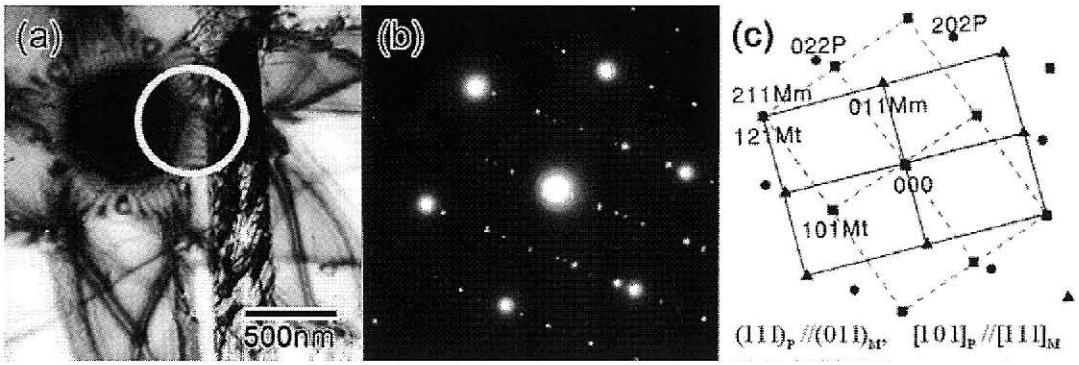

Fig. 2-6 A transmission electron micrograph showing α′ martensite formed in a sensitized (100 h) SUS304 stainless steel (a), the diffraction pattern taken from encircled area (b) and its schematic illustration (c). The diffraction pattern includes reflections form γ-phase (P), matrix of α′ martensite (Mm) and its twin (Mt). The γ-phase and α′-martensite satisfy the K-S relation.

SUS304L stainless steel after isothermal holding at 77 K for 10^6 s. In the figure, a band is seen in the matrix of the γ-phase as indicated by 'A'. In addition, we notice some wedge-shaped plates inside the band as indicated by 'B'. Considering previous report[30], we know that the banded plate indicated by 'A' is due to the formation of ε′-martensite and the wedge-shaped

plates correspond to the α′-martensite. Similar results have been obtained in a sensitized SUS304 and SUS304L stainless steels after isothermal holding. Then, we speculate that the isothermal martensitic transformation sequence of the solution-treated SUS304L, sensitized SUS304 and SUS304L stainless steels is $\gamma \rightarrow \varepsilon' \rightarrow \alpha'$. In the sensitized SUS304 and SUS304L stainless steels, however, we found that direct $\gamma \rightarrow \alpha'$ transformation occurs during isothermal holding at 77 K. A typical microstructure is shown in Fig. 2-5. The wedge-shaped plates of the α′-phase are formed in the γ-phase. Also, we have observed the direct $\gamma \rightarrow \alpha'$ transformation by TEM. Figure 2-6 (a) shows a TEM micrograph of the α′ martensite formed in the matrix (γ-phase) of a sensitized SUS304 stainless steel. From the diffraction pattern (b) and its schematic illustration (c), we know that the orientation relationship between α′ and γ satisfies the Kurdjumov–Sachs relation[31], which is characteristic to the direct $\gamma \rightarrow \alpha'$ transformation observed in many steels.

2.3.2 Effect of magnetic field on transformation behavior

We have investigated the effect of high magnetic field on martensitic transformation for the all steels. In order to examine the effect of high magnetic field on the transformation of single γ-phase state, we applied pulsed high magnetic field of up to 30 MA/m at 4.2 K ($<T_N$) and at 77 K ($>T_N$) of single γ-phase state, and found that no magnetic field-induced transformation occurs for all steels at these temperatures.

Next, in order to examine the effect of high magnetic field on the $\varepsilon' \rightarrow \alpha'$ transformation, we have applied a pulsed high magnetic field at room temperature to a solution-treated SUS304L in a mixed state of γ-, ε′- and α′-phases, state of which was formed beforehand by isothermal holding at 77 K for 10^6 s. Figure 2-7 shows magnetization curve obtained at R.T. in a low field range of the solution-treated SUS304L before (a) and after (b) a high magnetic field application (30 MA/m at 77 K). Obviously, the spontaneous magnetization is increased by the high field application, meaning that the α′-phase is further induced from the ε′-phase by magnetic field. The change in the fraction of α′-phase by the high filed application is about 0.3 %. Similar result was obtained for the sensitized SUS304 and SUS304L stainless steels.

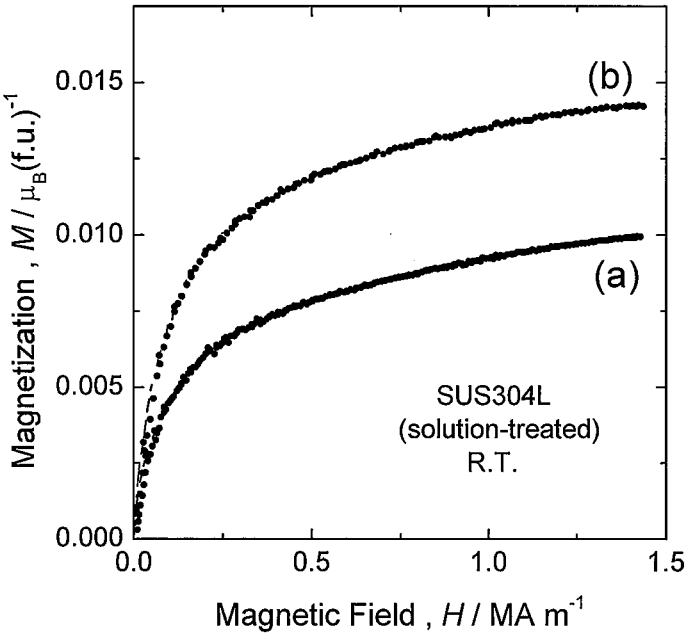

Fig. 2-7 Magnetization curves at room temperature of a solution-treated SUS304L stainless steel (a) before and (b) after a high magnetic field application (30 MA/m at 77 K). Prior to the high field application, the specimen has experienced isothermal holding at 77 K for 10^6 s.

The different influence of magnetic field on $\gamma \rightarrow \varepsilon' \rightarrow \alpha'$ and $\varepsilon' \rightarrow \alpha'$ transformations will be discussed later.

2.3.3 Effect of deformation under a uniaxial stress on transformation behavior

We have carried out tensile tests on the present steels with the solution-treated and sensitized states, and evaluated the amount of deformation-induced martensite. The magnetization curves obtained at 77 K for a solution-treated SUS304L stainless steel deformed at 77 K by 5 % and 30 % (nominal strain) are shown in Fig. 2-8 (a) and (b), respectively. The spontaneous magnetization of these curves is due to deformation-induced α'-phase. Similar results were obtained in all the steels. We can evaluate the fraction of α'-martensite by the same method mentioned in section 2.3.1. In here, the values of $M_0^{\alpha'}(0)$ for SUS316 and SUS316L stainless steels are estimated to be 1.70 and 1.90 μ_B/atom, respectively, considering the Slater-Pauling curve and their valence electron concentration[29]. The results are shown

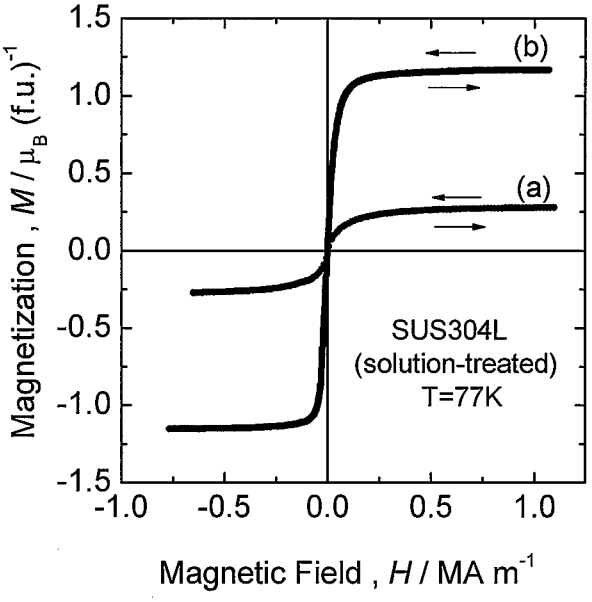

Fig. 2-8 Magnetization curves at 77 K for a solution-treated SUS304L stainless steel deformed at 77 K by 5% (a) and 30% (b).

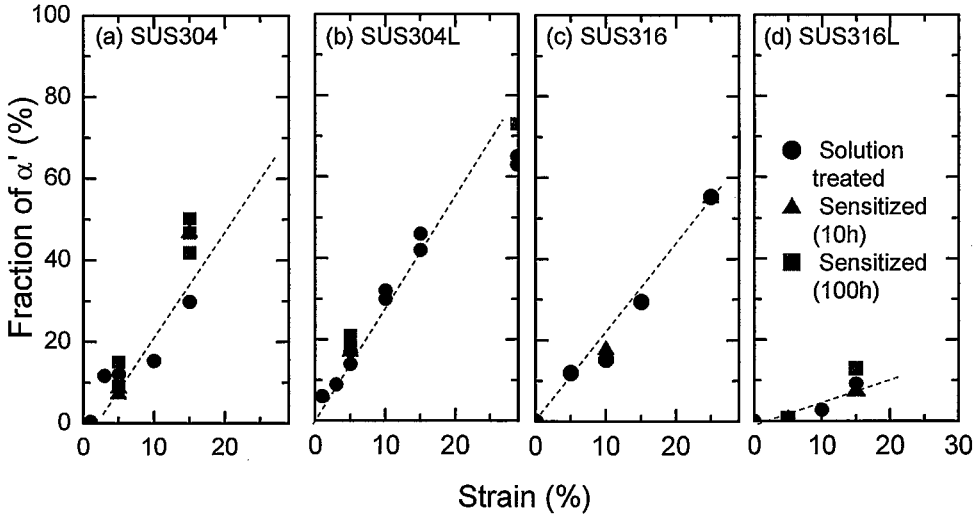

Fig. 2-9 Volume fraction of strain-induced α'-martensite at 77 K in the solution-treated and sensitized SUS304, SUS304L, SUS316 and SUS316L stainless steels. Lines are guide for eyes.

in Fig. 2-9 for all the solution-treated and sensitized stainless steels. The amount of α'-martensite increases with increasing strain, but it does not depend on the effect of sensitization. In order to investigate the transformation sequence of deformation-induced martensite, we have

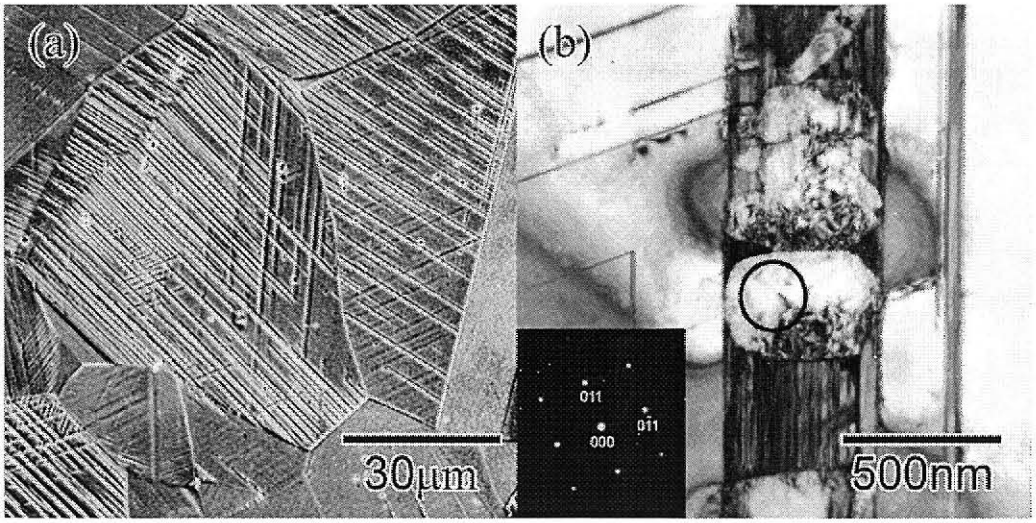

Fig. 2-10 SEM (a) and TEM (b) observation of a solution-treated SUS304L stainless steel deformed by 1% at 77 K.

made SEM and TEM observations. Figure 2-10 shows SEM (a) and TEM (b) observation results obtained at R.T. in solution-treated SUS304L stainless steel deformed at 77 K by 1 %. In figure (a), we notice banded plates which corresponds to the ε′-phase formed in the γ-phase. Figure 2-10 (b) shows the bright field image of an ε′-plate. We notice some particles in the ε′-plate. From the electron diffraction pattern corresponding to the encircled area, this particle is confirmed to be the α′-phase. The same microstructure was observed in all the solution-treated and sensitized stainless steels. From these results, deformation-induced transformation sequence is confirmed to be $\gamma \rightarrow \varepsilon' \rightarrow \alpha'$ for all the steels. It should be noted that the thickness of deformation-induced ε′ plate is very thin compared with that of isothermally induced ε′ shown in Fig. 2-4.

2.3.4 Effect of combined environment on transformation behavior

In order to examine the martensite transformation behavior under a combined environment of high magnetic field and deformation, we have applied a high magnetic field at 77 or 4.2 K on the present steels which were beforehand deformed at 77 K, and examined the change of the amount of α′-martensite. Figure 2-11 (a) is an example showing the effect of high magnetic field of 27.8 MA/m at 77 K for a solution-treated SUS304L stainless steel deformed beforehand

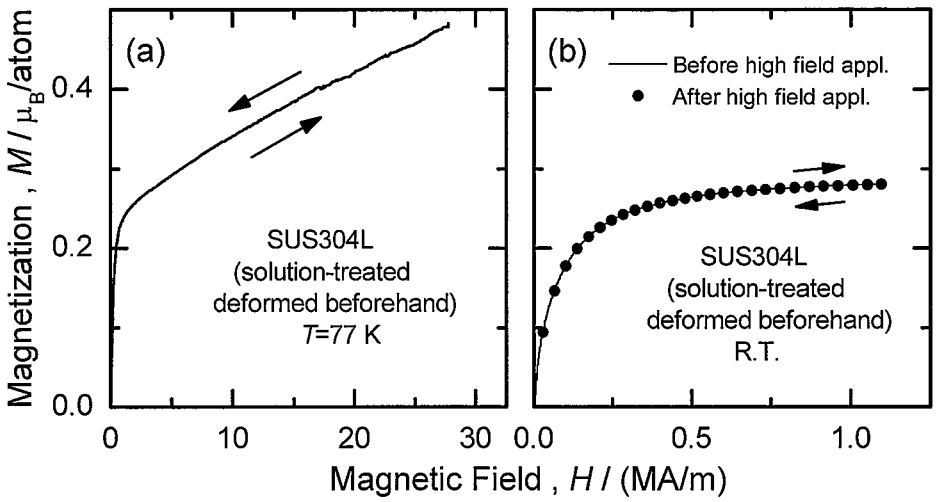

Fig. 2-11 Magnetization curve at 77 K of a solution-treated SUS304L stainless steel under a pulsed high magnetic field (a), and magnetization curve at room temperature in a low field region before and after the high field application (b). Prior to high field application, the specimen was worked by 5% at 77 K.

by 5 % at 77 K. As known from (a), there is neither abrupt increase in magnetization nor hysteresis in the curve. This result means that the α′-martensite is not formed by the high field application in the specimen. This fact can be also confirmed by magnetization curves at room temperature in a low field region measured before and after the high field application (Fig. 2-11 (b)). The two magnetization curves completely coincide, meaning no increase in the fraction of the α′-phase. Similar results are obtained for all the solution-treated and sensitized steels which were deformed beforehand 10, 15 and 30 % at 77 K and/or 4.2 K.

2.4 Discussion

The present results for the phase stability of solution-treated and sensitized SUS304, SUS304L, SUS316 and SUS316L stainless steels under external fields (cryogenic temperature, high magnetic field, deformation and combination of them) are summarized in Table 2-2.

Table 2-2. Martensitic transformation sequence in austenitic stainless steels induced by isothermal holding at 77 K (IH), by an application of a high magnetic field without isothermal holding (HMF), by an application of a high magnetic field at 77 K after isothermal holding (IH → HMF), by deformation at 77 K (DF), and by an application of a high magnetic field after deformation (IH → HMF).

Type	**IH**	**HMF**	**IH → HMF**	**DF**	**DF → HMF**
SUS304 (T)	NI	NI	NI	$\gamma \rightarrow \varepsilon' \rightarrow \alpha'$	NI
SUS304 (S)	$\gamma \rightarrow \varepsilon' \rightarrow \alpha'$ $\gamma \rightarrow \alpha'$	NI	$\varepsilon' \rightarrow \alpha'$	$\gamma \rightarrow \varepsilon' \rightarrow \alpha'$	NI
SUS304L (T)	$\gamma \rightarrow \varepsilon' \rightarrow \alpha'$	NI	$\varepsilon' \rightarrow \alpha'$	$\gamma \rightarrow \varepsilon' \rightarrow \alpha'$	NI
SUS304L (S)	$\gamma \rightarrow \varepsilon' \rightarrow \alpha'$ $\gamma \rightarrow \alpha'$	NI	$\varepsilon' \rightarrow \alpha'$	$\gamma \rightarrow \varepsilon' \rightarrow \alpha'$	NI
SUS316 (T)	NI	NI	NI	$\gamma \rightarrow \varepsilon' \rightarrow \alpha'$	NI
SUS316 (S)	NI	NI	NI	$\gamma \rightarrow \varepsilon' \rightarrow \alpha'$	NI
SUS316L (T)	NI	NI	NI	$\gamma \rightarrow \varepsilon' \rightarrow \alpha'$	NI
SUS316L (S)	NI	NI	NI	$\gamma \rightarrow \varepsilon' \rightarrow \alpha'$	NI

From the summary, we know the following:

(i) The α′-martensite is not induced by the application of the magnetic field from a solution-treated γ-phase.

(ii) Although the α′-martensite is induced by magnetic field in the ε′-martensite formed beforehand by isothermal transformation, it is not induced by magnetic field in the ε′-martensite formed beforehand by deformation.

We first discuss the reason of (i). Since both γ- and ε′-phase are nonmagnetic, the change in free energy by magnetic field is small for both the phases, and consequently the $\gamma \rightarrow \varepsilon'$ transformation will not be induced by application of magnetic field. As a result, the $\gamma \rightarrow \varepsilon' \rightarrow \alpha'$ transformation is not induced by the application of magnetic field. For further discussion, magnetic properties of ε′-martensite are needed.

Next we discuss the reason of (ii). Since the α′-martensite is ferromagnetic and ε′-martensite is nonmagnetic, the free energy of the α′-martensite decreases compared with the ε′-martensite by the application of magnetic field. Then the α′-martensite can be induced by magnetic field, and actually it is induced in the ε′-martensite formed by isothermal holding of the solution-treated SUS304L, sensitized SUS304 and SUS304L stainless steels as described in Fig. 2-7. On the other hand, the α′-martensite was not induced from the ε′-martensite formed by deformation in the same steel. The difference can not be explained by only the magnetic energy. The thickness of the ε′-plate should be considered to understand the difference. As described previously, the ε′-plate induced by deformation is very thin compared with that induced by isothermal holding. The formation of the α′-martensite from the thin ε′-plate will be suppressed due to the grain size effect, which is the effect that martensitic transformation temperature decrease with decreasing grain size in many steels[32-36]. Presumably, higher magnetic field is required to induce the α′-martensite in the thin ε′-plate formed by deformation.

2.5 Conclusions

We have investigated effects of cryogenic temperature, high stress and high magnetic field on martensitic transformation in SUS304, SUS304L, SUS316 and SUS316L austenitic stainless steels, and the following results are obtained.

(1) No athermal martensitic transformation occurs in all the solution-treated and sensitized stainless steels. On the contrary, isothermal transformation occurs in the sensitized

SUS304 (($\gamma \rightarrow \varepsilon' \rightarrow \alpha'$ and $\gamma \rightarrow \alpha'$) between about 150 and 250 K. It also occurs in the solution-treated ($\gamma \rightarrow \varepsilon' \rightarrow \alpha'$) and sensitized SUS304L ($\gamma \rightarrow \varepsilon' \rightarrow \alpha'$ and $\gamma \rightarrow \alpha'$) between about 70 and 170 K.

(2) The γ-phase exhibits an antiferromagnetic transition at about 40 K in all the stainless steels.

(3) Deformation-induced $\gamma \rightarrow \varepsilon' \rightarrow \alpha'$ martensitic transformation occurs at 77 K in all the solution-treated and sensitized steels.

(4) Magnetic field-induced martensite transformation does not occur in the γ-phase even when the pulsed magnetic field of up to 30 MA/m is applied in the wide temperature range between 4.2 and 290 K.

(5) Magnetic field-induced martensitic transformation ($\varepsilon' \rightarrow \alpha'$) occurs in the solution-treated SUS304L, sensitized SUS304 and SUS304L which contains isothermally transformed ε'-martensite. However it does not occur when ε'-martensite is formed by deformation.

References

[1] D. C. Larbalestier and H.W. King, *Cryogenics* **13** (1973) 160

[2] D. T. Read and R. P. Reed, *Cryogenics* **21** (1981) 415

[3] T. Tanaka, T. Kadota, Y. Kohno and K. Shibata, *Adv. Cryogenic Engng. Mater.* **44** (1998) 1

[4] N. Yasumaru, *Mater. Trans.* **39** (1998) 1046

[5] S. Murase, S. Kobatake, M. Tanaka, I. Tashiro, O. Horigami, H. Ogiwara, K. Shibata, K. Nagai and K. Ishikawa, *Fusion Eng. Des.* **20** (1993) 451

[6] J. W. Chan, D. Chu, A. J. Sunwoo and J. W. Morris, Jr., *Adv. Cryogenic Engng. Mater.* **38** (1992) 55

[7] B. Cina, J. Iron Steel Inst. **177** (1954) 406

[8] R.P. Reed, *Acta Metall.* **10** (1962) 865

[9] Pat L. Mangonon Jr., G. Thomas, *Metall. Trans.* **1** (1970) 1577

[10] S. S. Hecker, M. G. Stout, K. P. Staudhammer and J. L. Smith, *Metall. Trans. A* **13A** (1982) 619

[11] T. Shimozono, Y. Kohno, H. Konishi, K. Shibata, H. Ohtsuka and H. Wada, *Mater. Sci. Eng. A* **273-275** (1999) 337

[12] H. C. Shin, T. K. Ha and Y. W. Chang, *Scripta Mater.* **45** (2001) 823

[13] K. Mumtaz, S. Takahashi, J. Echigoya, L. F. Zhang, Y. Kamada and M. Sato, *J. Mater. Sci.* **38** (2003) 3037

[14] E. Nagy, V. Mertinger, F. Tranta and J. Sólyom, *Mater. Sci. Eng. A* **378** (2004) 308

[15] K. Mumtaz, S. Takahashi, J. Echigoya, Y. Kamada, L. F. Zhang, H. Kikuchi, K. Ara and M. Sato, *J. Mater. Sci.* **39** (2004) 1997

[16] L. Zhang, S. Takahashi, Y. Kamada, H. Kikuchi, K. Ara, M. Sato and T. Tsukada, *J. Mater. Sci.* **40** (2005) 2709

[17] B. Fultz and J. W. Morris Jr, *Acta Metall.* **34** (1986) 379

[18] R. B. Goldfarb, R. P. Reed, J. W. Ekin and J. M. Arvidson, *Adv. Cryogenic Engng. Mater.* **30** (1984) 475

[19] D. N. Bolshutkin, V. A. Desnenko and V. Ya. Ilichev, *Cryogenics* **19** (1979) 231

[20] B. I. Verkin, V. Ya. Ilichev and I. N. Klimenko, *Adv. Cryogenic Engng. Mater.* **26** (1980) 120

[21] L. Mangonon Jr. and G. Thomas, *Metall. Trans.* **1A** (1970) 1577

[22] G. B. Olson and M. Cohen, *Metall. Trans.* **6A** (1975) 791

[23] T. Suzuki, H. Kojima, K. Suzuki, T. Hashimoto and M. Ichihara, *Acta Metall.* **25** (1977) 1151

[24] U. Gonser, C. J. Meechan, A. H. Muir and H. Wiedersich, *J. Appl. Phys.* **34** (1963) 2373

[25] F. De Backer, V. Schoss and G. Maussner, *Nucl. Eng. Des.* **206** (2001) 201

[26] A. Miller, Y. Estrin and X. Z. Hu, *Scripta Mater* **47** (2002) 441

[27] A. Mitra, P. K. Srivastava, P. K. De, D. K. Bhattacharya and D. C. Jiles, *Metall. Mater. Trans. A* **35A** (2004) 559

[28] Y. Kamada, T. Mikami, S. Takahashi, H. Kikuchi, S. Kobayashi and K. Ara, *J. Magn. Magn. Mater.* **310** (2007) 2856

[29] J. Crangle and G. C. Hallam, *Proc. Poy. Soc.* **A272** (1963) 119

[30] A. K. De, D. C. Murdock, M. C. Mataya, J. G. Speer and D. K. Matlock, *Scr. Mater.* **50** (2004) 1445

[31] D. B. Williams and C. B. Carter: *Transmission Electron Microscopy* (Plenum Press, New York, 1996) pp. 285

[32] D. N. Adnyana, *Metallography* **19** (1986) 187

[33] W. Jianxin, J. Bohong and T. Y. Hsu, *Acta Metall.* **36** (1988) 1521

[34] G. L. Huang, D. K. Matlock and G. Krauss, *Metall. Trans. A* **20** (1989) 1239

[35] B. H. Jiang, L. Sun, R. Li and T. Y. Hsu, *Scripta Metall.* **33** (1995) 63

[36] S. F. Peterson, M. C. Mataya and D. K. Matlock, *JOM* **49** (1997) 54

Chapter 3

Time-temperature-transformation diagram of isothermal martensitic transformation in solution-treated SUS304L stainless steel

3.1 Introduction

Martensitic transformations are well known to be classified into two groups with respect to kinetics[1-3], as mentioned in section 1.3.3. One is athermal transformation and the other is isothermal transformation. The former transformation has a definite martensitic transformation start temperature, M_s, and occurs instantaneously when the temperature reaches the M_s in the cooling process. One the other hand, the latter does not have a definite M_s but occurs after some finite incubation time during isothermal holding at a constant temperature, and the amount of martensite phase increases with increasing the isothermal holding time. Although such two kinds of transformations kinetics are now basically explained by a universal phenomenological theory[4-5], the number of alloys exhibiting an obvious isothermal transformation is small. For this reason, most of the isothermal transformations studied so far are the $\gamma \rightarrow \alpha'$ ones observed in Fe-Ni-Cr and Fe-Ni-Mn alloys[6-12]. The isothermal transformation in these alloys is characterized by a C-curve in time-temperature-transformation (*TTT*) diagram.

In chapter 2, however, we found a new type of isothermal martensitic transformation in a solution-treated SUS304L stainless steel. In this steel, the successive $\gamma \rightarrow \varepsilon' \rightarrow \alpha'$ martensitic transformation proceeded by isothermal holding at 77 K. As far as the authors are aware, this was the first finding of isothermal successive $\gamma \rightarrow \varepsilon' \rightarrow \alpha'$ martensitic transformation. However, we examined the isothermal transformation only at 77 K, and the *TTT* diagram of isothermal martensitic transformation has not been constructed yet.

In this chapter, therefore, we examine the isothermal transformation of the solution-treated SUS304L stainless steel in the temperature range between 70 and 170 K, and construct the *TTT* diagram of the successive $\gamma \rightarrow \varepsilon' \rightarrow \alpha'$ martensitic transformation.

3.2 Experimental Procedure

The chemical composition of SUS304L stainless steel used in this chapter is the same as that shown in Table 2-1. Details of alloy production and specimen preparation were the same as described in chapter 2. Specimens of 3 × 3 × 1 mm in size were cut out, and were solution-treated at 1323 K for 0.5 h in vacuum followed by quenching into iced water.

Isothermal holding experiments of the specimens were carried out in the temperature range between 70 and 170 K for various times. The volume fraction of the α'-martensite, $f_{\alpha'}$, formed by the isothermal holding was evaluated by a magnetization measurement at 300 K (= T_R). Details of this measurement were described in chapter 2.

The variation of morphologies was observed by *In-situ* optical microscopy (OM) during the isothermal holding experiment. Temperature of the specimen was regulated by controlling the evaporation of liquid N_2. After isothermal holding experiment, the microstructure was investigated by *in-situ* transmission electron microscopy (TEM). Specimens for TEM observation were prepared by electropolishing using an electrolyte consisting of 85 % CH_3COOH and 15 % $HClO_4$ in volume. TEM observation was made with an accelerating voltage of 200 kV.

3.3 Results and Discussion

3.3.1 TTT diagram for the successive $\gamma \rightarrow \varepsilon' \rightarrow \alpha'$ martensitic transformation

First of all, martensitic transformation behavior and magnetic properties of the present

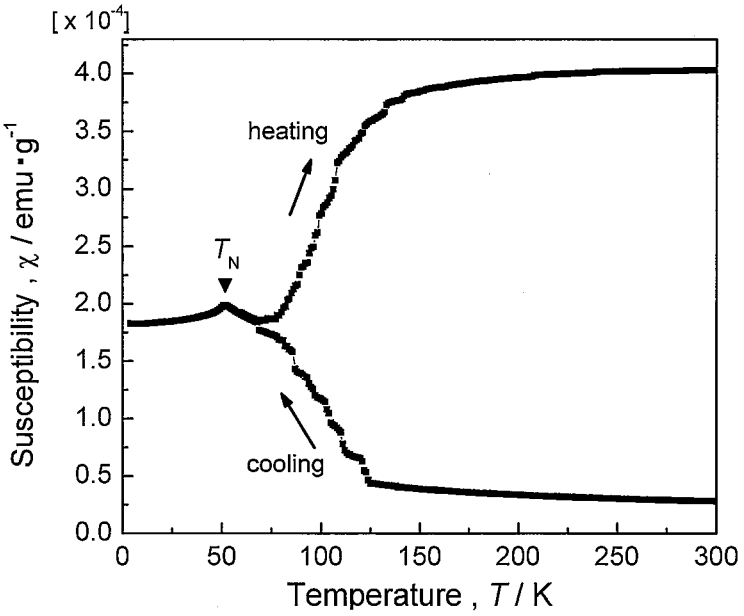

Fig. 3-1 Magnetic susceptibility curve of the solution-treated SUS304L stainless steel measured in the cooling and heating processes.

SUS304L stainless steel has been checked by magnetic susceptibility measurement. Figure 3-1 shows temperature dependence of magnetic susceptibility, χ, of the solution-treated SUS304L stainless steel. In the cooling process, the magnetic susceptibility increases in the temperature range between 70 and 170 K. A characteristic feature is that it also increases in the heating

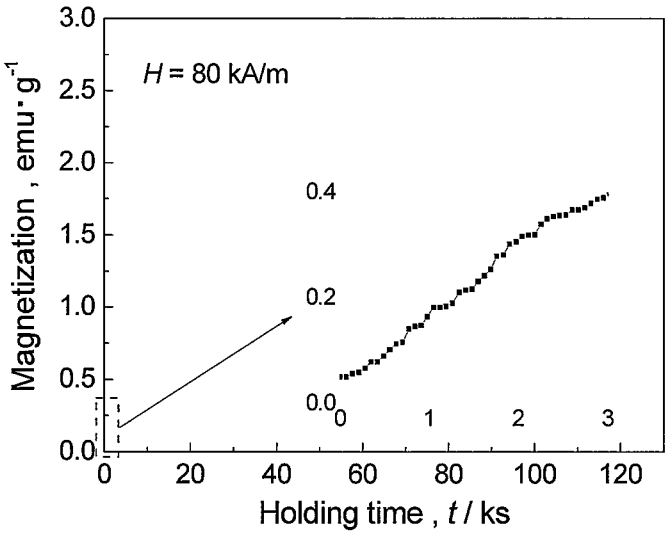

Fig. 3-2 Relation between magnetization of the specimen and holding time at 103 K in the solution-treated SUS304L stainless steel. The inset is the magnification of the dotted area.

process in the same temperature range. Such increase in magnetic susceptibility is due to the formation of ferromagnetic α′-phase, meaning that isothermal γ → ε′ → α′ martensitic transformation occurs in the present specimen, being in good agreement with the result described in chapter 2 fig. 2-1 (b). The isothermal kinetics of the successive martensitic transformation is due to the γ → ε′ martensitic transformation, which will be described later. Incidentally, the Néel temperature (indicated by T_N) of the residual γ-phase also agrees with previous specimen studied in chapter 2.

Next, the time evolution of α′-martensite during isothermal holding at 103 K has been examined by magnetization measurement under a low magnetic field of 80 kA/m, and the result is shown in Fig. 3-2. The magnetization increases linearly with increasing holding time at the initial stage, and then the increasing-ratio decreases in the long time range of holding. A characteristic feature is that if we magnify the curve (inset of Fig. 3-2), we notice a

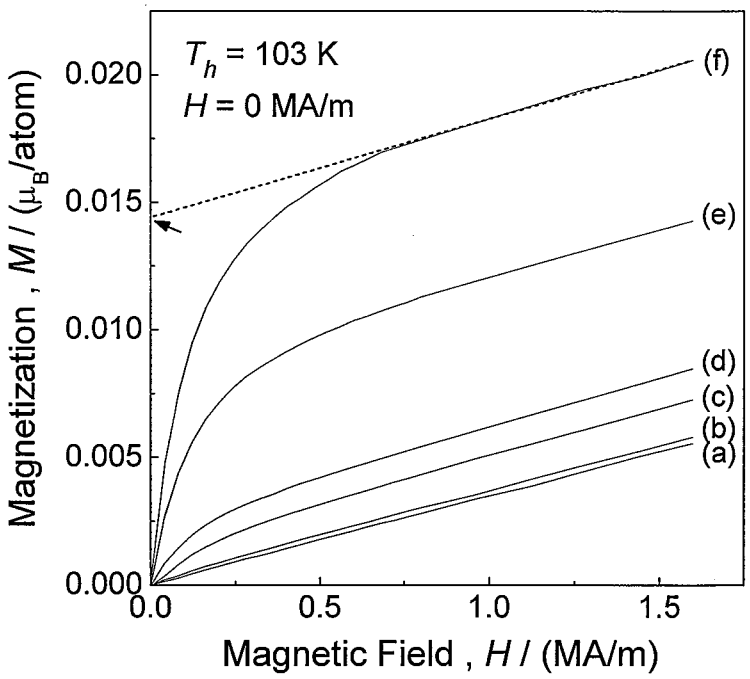

Fig. 3-3 Magnetization curves at 300 K of the solution-treated SUS304L stainless steel after isothermal holding measurement at 103 K for (a) 50 s, (b) 170 s, (c) 520 s, (d) 1660 s, (e) 5200 s and (f) 10400 s, respectively.

discontinuous or a step-like increase in magnetization during the isothermal holding process. This result means that increase in the fraction of α′-martensite occurs instantaneously and step by step.

Isothermal holding experiment for obtaining the *TTT* curve has been carried out in the absent of magnetic field at several temperatures in the temperature range between 70 and 170 K. Figure 3-3 shows magnetization curves at T_R = 300 K after isothermal holding at 103 K for 50 s (a), 170 s (b), 520 s (c), 1660 s (d), 5200 s (e) and 10400 s (f). We can evaluate the spontaneous magnetization from these curves. As an example, the spontaneous magnetization obtained from curve (f) is indicated with an arrow in Fig. 3-3. Obviously, the spontaneous magnetization increases with increasing the isothermal holding time.

The volume fraction of α′-martensite ($f_{\alpha'}$) can be evaluated from the spontaneous magnetization as described in experimental procedure, and the volume fraction thus obtained is plotted with solid circles as a function of holding time in Fig. 3-4. The same experiments have

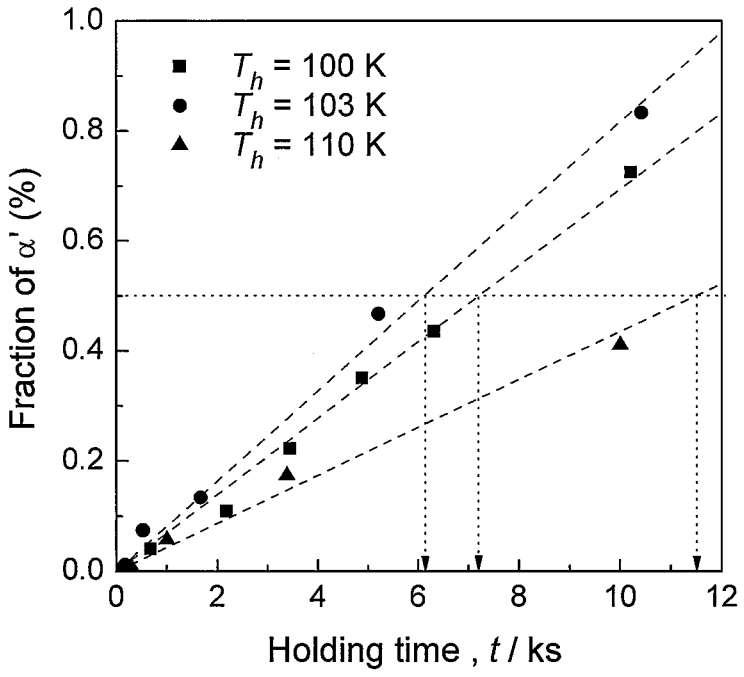

Fig. 3-4 Volume fraction of α′-martensite at various temperatures in the solution-treated SUS304L stainless steel. Dashed lines are guide for eyes.

been made at 116, 110, 105, 100, 95 and 87 K, and the results at 100 and 110 K are also shown in Fig. 3-4. We know from the result that the $f_{\alpha'}$ obviously depends on holding temperature as well as holding time. Incidentally, as known from Fig. 3-4, the magnetization increases linearly with increasing holding time. Such a linear increase of $f_{\alpha'}$ is due to small amount of α′-martensite formed in initial stage of isothermal holding.

From the linear relation shown in Fig. 3-4, the time required for the formation of 0.5 vol. % of α′-martensite is obtained. It is 7.1 ks at 100 K, 6.1 ks at 103 K and 12.6 ks at 110 K as shown by arrows. Using these times, we have constructed the *TTT* diagram of 0.5 vol. % of α′-martensite as shown in Fig. 3-5. The results at 116, 105, 95 and 87 K obtained by the same method are also plotted in Fig. 3-5. It should be noted in this result that *TTT* diagram clearly forms a typical C-curve, and nose temperature (indicated by an arrow) is about 103 K.

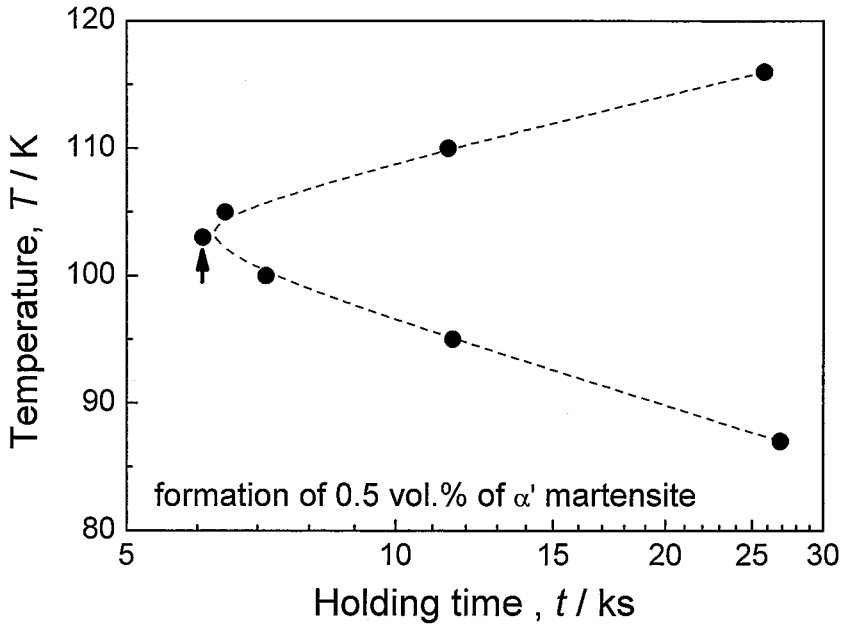

Fig. 3-5 *TTT* diagram of the isothermal martensitic transformation in the solution-treated SUS304L stainless steel, and dashed line is guide for eyes.

3.3.2 Morphologies of martensites formed during isothermal holding

In order to know how the isothermal $\gamma \rightarrow \varepsilon' \rightarrow \alpha'$ martensitic transformation proceeds, we have made *in-situ* optical microscope observation. Figure 3-6 shows a series of optical micrographs showing isothermal $\gamma \rightarrow \varepsilon' \rightarrow \alpha'$ martensitic transformation at 103 K. After isothermal holding of 3×10^2 s, banded plates of the ε'-martensite appeared in the matrix of the γ-phase as indicated by 'A' in Fig. 3-6 (a). The number of ε'-plates gradually increases with increasing holding time as seen in (b) and (c). In addition, the constant of the γ-phase enclosed by banded ε'-plates (indicated by a dashed rectangle in Fig 3-6 (b)) also increases with increasing the holding time. Such a change in contrast will be due to the gradual growth of banded ε'-martensites. That is, the $\gamma \rightarrow \varepsilon'$ martensitic transformation proceeds isothermally. On the other hand, Fig. 3-6 (d) shows that wedge-shaped plates, which are characteristics of α' martensite[13-14], instantaneously forms in the banded ε'-plates as indicated by 'B'. The α'-martensite thus formed does not grow by increasing the isothermal holding time. This result

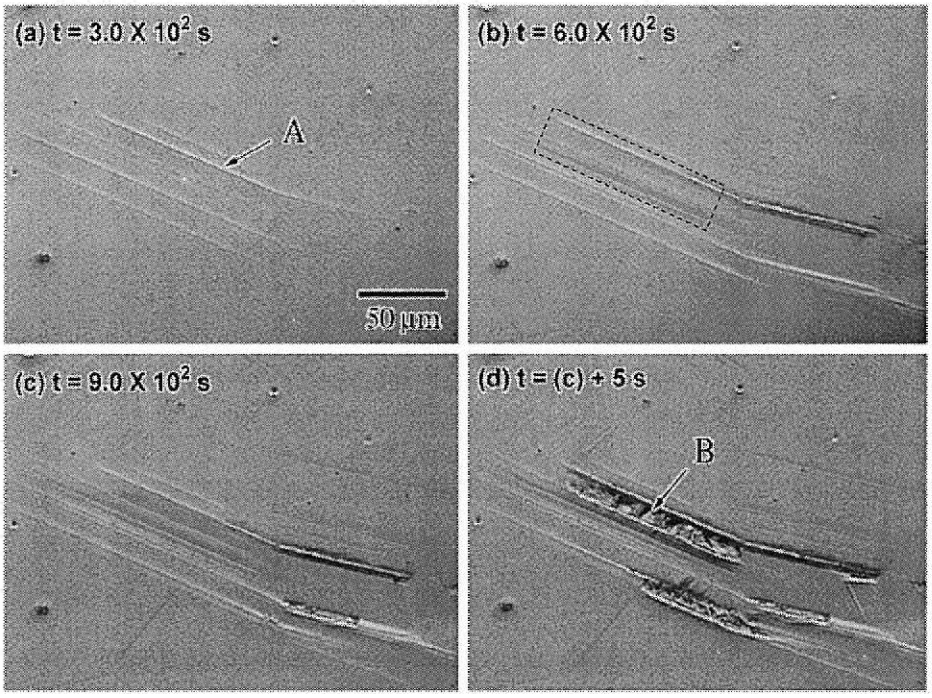

Fig. 3-6 A series of *in-situ* optical micrographs of the solution-treated SUS304L stainless steel showing successive $\gamma \rightarrow \varepsilon' \rightarrow \alpha'$ martensitic transformation at 103 K.

suggests that the $\varepsilon' \rightarrow \alpha'$ martensitic transformation is athermal one.

It is likely form the optical microscope observation that the successive $\gamma \rightarrow \varepsilon' \rightarrow \alpha'$ martensitic transformation proceeds by an isothermal $\gamma \rightarrow \varepsilon'$ martensitic transformation followed by an athermal $\varepsilon' \rightarrow \alpha'$ martensitic transformation. If this interpretation is appropriate, the C-curve nature of the *TTT* diagram in Fig. 3-5 is essentially due to the kinetics of $\gamma \rightarrow \varepsilon'$ martensitic transformation although the curve is experimentally obtained from the volume fraction of the α'-martensite.

To understand the martensitic transformation mechanism in the solution-treated SUS304L stainless steel, the microstructure of ε'- and α'-phase formed by isothermal holding was examined by using *in-situ* TEM. Figure 3-7 shows a bright filed image after isothermal holding at 103 K for 2 h. In this result, we can see the morphologies of ε'- and α'-martensite indicated by "A" and "B" respectively. We notice from this observation that the ε'-martensites were composed of layered slip bands and some of the vertical slip bands, and there exist intersections of two kinds of slip bands as indicated typically by an arrow. This

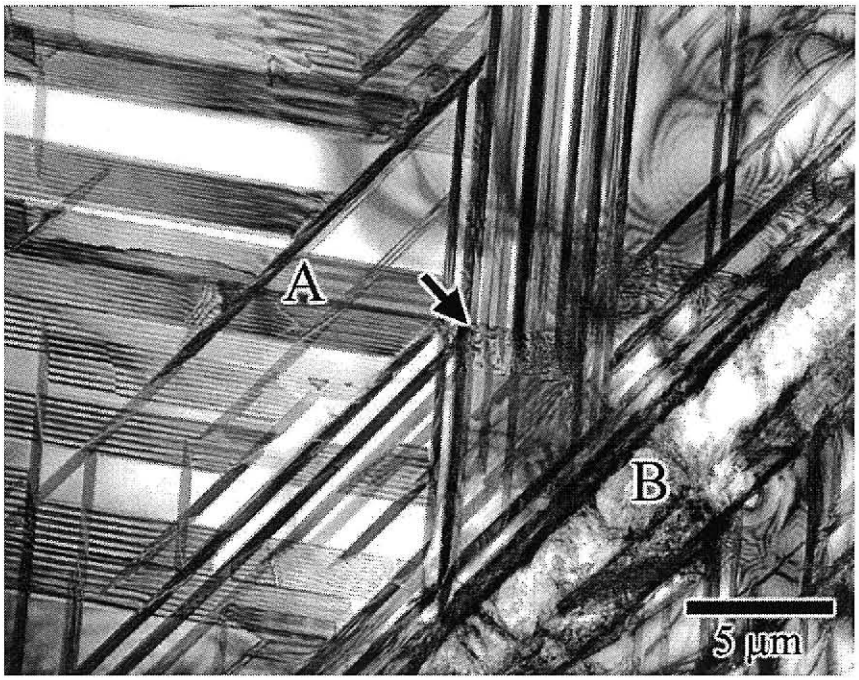

Fig. 3-7 *In-situ* TEM observation result of the solution-treated SUS304L stainless steel after isothermal holding at 103 K for 2 h.

microstructural morphology formed by isothermal holding is similar to that of tensile deformed specimens of some austenitic stainless steels in the previous studies[15-22]. In the case of the deformation induced martensitic transformation, it was commonly known that embryo of the α′-martensite is created at the intersection of two slip bands. That is, the α′-martensitic transformation occurs at the intersection of slip bands when the slip bands are composed of either ε′-martensite or a dense collection of layered staking faults. From this result, we suggest that the ε′ → α′ martensitic transformation may occur at the intersection of the banded ε′-martensite during the isothermal holding.

3.4 Conclusions

We have investigated *TTT* diagram of isothermal martensitic transformation in a solution-treated SUS304L stainless steel and the following results have been obtained.

(1) Successive γ → ε′ → α′ martensitic transformation probably proceeds by so-called isothermal γ → ε′ martensitic transformation followed by so-called athermal ε′ → α′ martensitic transformation.

(2) *TTT* diagram of the successive γ → ε′ → α′ martensitic transformation shows a C-curve with a nose temperature located at about 103 K due to the isothermal nature of the γ → ε′ martensitic transformation.

References

[1] G. V. Kurdjumov and O. P. Maksimova, *Dokl. Akad. Nauk SSSR* **61** (1948) 83

[2] G. V. Kurdjumov and O. P. Maksimova, *Dokl. Akad. Nauk SSSR* **73** (1950) 95

[3] S. Kajiwara, *Acta Metall.* **32** (1984) 407

[4] T. Kakeshita, K. Kuroiwa, K. Shimizu, T. Ikeda, A. Yamagishi and M. Date, *Mater. Trans. JIM* **34** (1993) 423

[5] T. Kakeshita, T. Saburi and K. Shimizu, *Mater. Sci. Eng. A* **273-275** (1999) 21

[6] S. Kajiwara, *Philos. Mag. A* **43** (1981) 1483

[7] S. Kajiwara, *Mater. Trans. JIM* **33** (1992) 1027

[8] T. Kakeshita, K. Shimizu, M. Ono and M. Date, *Mater. Trans. JIM* **33** (1992) 461

[9] T. Kakeshita, K. Kuroiwa, K. Shimizu, T. Ikeda, A. Yamagishi and M. Date, *Mater. Trans. JIM* **34** (1993) 415

[10] T. Kakeshita, Y. Tomohiko, K. Shimizu, S. Sugiyama and S. Endo, *Mater. Trans. JIM* **36** (1995) 1018

[11] A. Borgenstam and M. Hillert, *Acta Mater.* **45** (1997) 651

[12] T. Kakeshita, Y. Sato, T. Saburi, K. Shimizu, Y. Matsuoka and K. Kindo, *Mater. Trans. JIM* **40** (1999) 100

[13] R. P. Reed, *Acta Metall.* **10** (1962) 865

[14] A. K. De, D. C. Murdock, M. C. Mataya, J. G. Speer and D. K. Matlock, *Scr. Mater.* **50** (2004) 1445

[15] G. B. Olson and M. Cohen, *Metall. Trans.* **6A** (1975) 791

[16] T. Suzuki, H. Kojima, K. Suzuki, T. Hashimoto and M. Ichihara, *Acta Metall.* **25** (1977) 1151

[17] J. W. Brooks, M. H. Loretto and R. E. Smallman, *Acta Metall.* **27** (1979) 1829

[18] J. W. Brooks, M. H. Loretto and R. E. Smallman, *Acta Metall.* **27** (1979) 1839

[19] T. Suzuku, M. Shimono and S. Kajiwara, *Mater. Sci. Eng. A* **312** (2001) 104

[20] T. Inamura, K. Takashima and Y. Higo, *Phil. Mag.* **83** (2003) 935

[21] K. Spencer, J. D. Embury, K. T. Conlon, M. Veron and Y. Brechet, *Mater. Sci. Eng. A* **387–389** (2004) 873

[22] L. Bracke, L. Kestens and J. Penning, *Scripta Mater.* **57** (2007) 385

Chapter 4

Time-temperature-transformation diagram of isothermal martensitic transformation in sensitized SUS304 stainless steel

4.1 Introduction

The austenitic stainless steels are characterized by good corrosion resistance, excellent mechanical properties, superior weldability and nonmagnetic characteristics[1-6], as mentioned in chapter 1. In particular, SUS304 stainless steel is extensively used in equipments for cryogenic applications such as tanks, piping system and other equipments for handling condensed gases. As mentioned in chapter 2, the austenitic stainless steels are unstable under some external fields, such as high stress and cryogenic temperature. Therefore, it is very important to clarify the stability of the austenite phase under such environments because many of the excellent properties could be deteriorated if the austenite phase transforms into martensite phases[7-10]. For example, the non-magnetic property of the austenite phase is lost when α'-martensite is formed[11-14], as described in chapter 2.

Generally, welding process is essential to use the austenitic stainless steel in various industries, and it is widely known that welded austenitic stainless steels can develop a sensitized zone which consists of carbide precipitation ($M_{23}C_6$) at grain boundaries and chromium depletion in the vicinity of grain boundaries[15-18]. In chapter 2, we found that the sensitized SUS304 stainless steel exhibits an isothermal martensitic transformation at cryogenic temperature. However, its time-temperature-transformation (*TTT*) diagram, which is one of the most important information for isothermal martensitic transformations, has not been constructed yet.

In this chapter, therefore, we have constructed the *TTT* diagram of the isothermal

martensitic transformation in a sensitized SUS304 stainless steel.

4.2 Experimental Procedure

The chemical composition of SUS304 stainless steel used in this chapter is the same as that shown in Table 2-1. The steel was cold-rolled into a sheet. From the sheet, specimens of 3 × 3 × 1 mm in size were cut out, and were solution-treated at 1323 K for 0.5 h in vacuum followed by quenching into iced water. Most of the specimens were sensitized by heat-treatment at 973 K for 100 h. Then the oxidized surface layer of all the specimens was eliminated by electropolishing, where an electrolyte composed of 85 % C_2H_5OH and 15 % $HClO_4$ in volume was used.

The microstructure of an as-sensitized specimen was observed by field emission scanning electron microscopy (FESEM). The etchant used for FESEM observation was 95 % H_2O_2 and 5 % HF in volume. As shown in Fig. 4-1, some particles of $M_{23}C_6$, confirmed by EDS analysis,

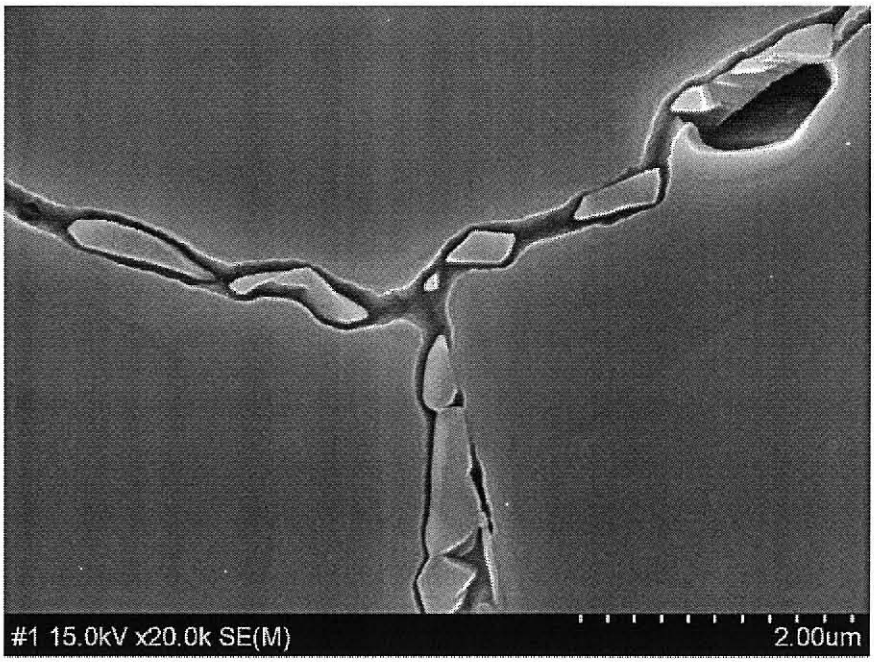

Fig. 4-1 FESEM observation result of a as-sensitized SUS304 stainless steel.

were observed along the grain boundaries. From this observation result, we know that the concentration of chromium between the inner region of grains and near grain boundaries is partially changed by the formation of $M_{23}C_6$ carbide. Such a change in chemical composition will affect in the martensitic transformation behavior between the inner region of grain and near grain boundaries.

Phase stability at cryogenic temperature was examined by the magnetic susceptibility measurement with a constant cooling and heating rate of 1 K/min in the temperature range between 4.2 and 300 K. Isothermal holding experiment was carried out under no magnetic field in the temperature range between 60 and 260 K for various holding times. The volume fraction of the α′-martensite, $f_{\alpha'}$, formed by the isothermal holding was evaluated by a magnetization measurement at 300 K (= T_R). Details of this method were described in chapter 2.

Change in morphology during the isothermal holding experiment was observed by *in-situ* optical microscopy (OM). Morphology of the martensite phase formed by isothermal holding experiment was investigated by transmission electron microscopy (TEM). Specimens for TEM observation were prepared by electropolishing using an electrolyte consisting of 85 % CH_3COOH and 15 % $HClO_4$ in volume. TEM observation was made with an accelerating voltage of 200 kV.

4.3 Results and Discussion

4.3.1 Construction of TTT diagram

In order to investigate the martensitic transformation and magnetic properties of the present SUS304 stainless steel, we have carried out magnetic susceptibility measurement in the temperature range between 4.2 and 300 K by applying a low magnetic filed of 79.6 kA/m. Figure 4-2 shows temperature dependence of magnetic susceptibility, χ, of the solution-treated and the sensitized SUS304 stainless steel. The χ–T curve of the solution-treated SUS304

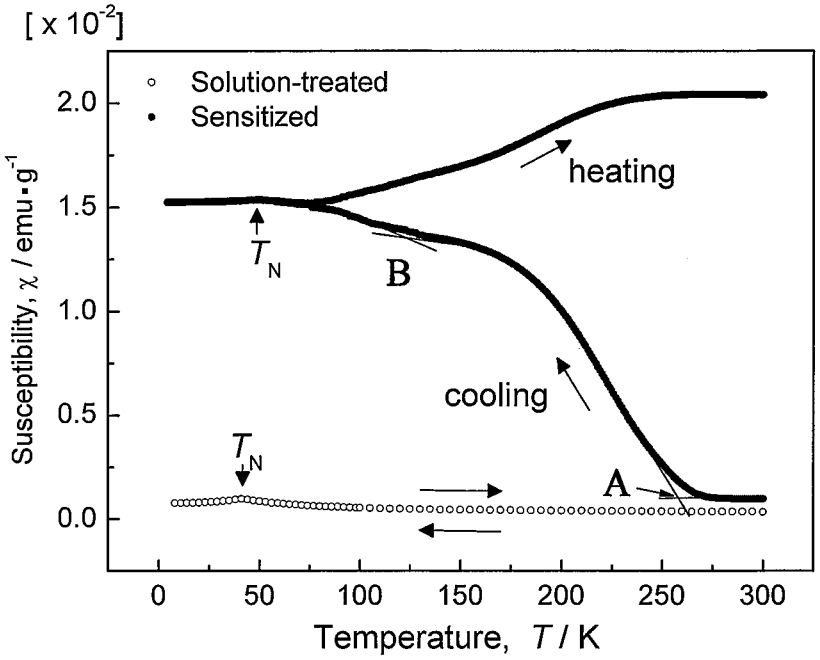

Fig. 4-2 Magnetic susceptibility curves of solution-treated and sensitized SUS304 stainless steel. Measurements were made in the cooling process and then in the heating process.

stainless steel shows a peak at about 40 K due to a paramagnetic to anti-ferromagnetic transition of the γ-phase and there is no hysteresis between heating and cooling processes, being in agreement with the result described in chapter 2. On the other hand, the χ–T curve of the sensitized SUS304 starts to increase at about 260 K in the cooling process as indicated with "A". Such increase of χ means that the ferromagnetic α′-martensite was formed during the cooling process. In the heating process, the χ–T curve starts to increase at about 60 K, meaning that the α′-martensite was also formed in the heating process. This result implies that the martensitic transformation of the sensitized SUS304 proceeds isothermally in the temperature range between 60 and 260 K. Furthermore, we notice that the χ–T curve increase in two step in the cooling process as indicated by "A" and "B", respectively. This result suggests that there exist two kinds of isothermal martensitic transformations in the sensitized SUS304 stainless steel.

In order to construct the *TTT* diagram, we have made isothermal holding experiment in the

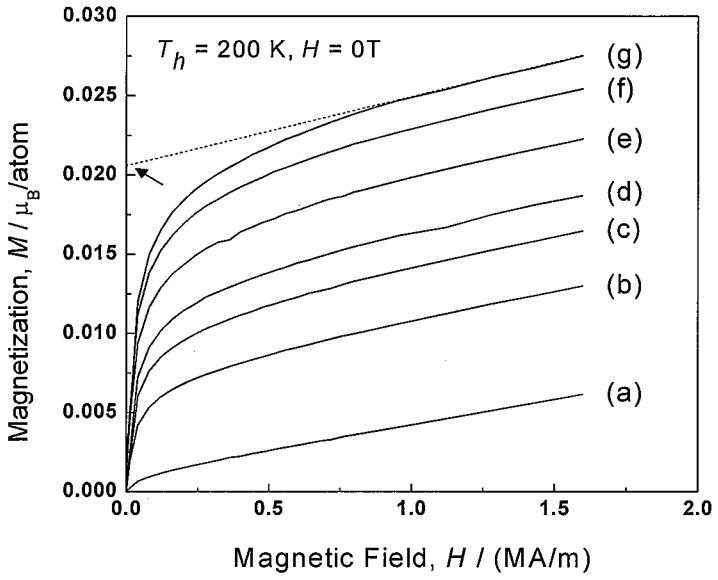

Fig. 4-3 Magnetization curves obtained at 300 K for the sensitized SUS304 stainless steel after isothermal holding at 200 K for 0 (a), 300 (b), 900 (c), 1800 (d), 3600 (e), 5400 (f) and 7200 s (g).

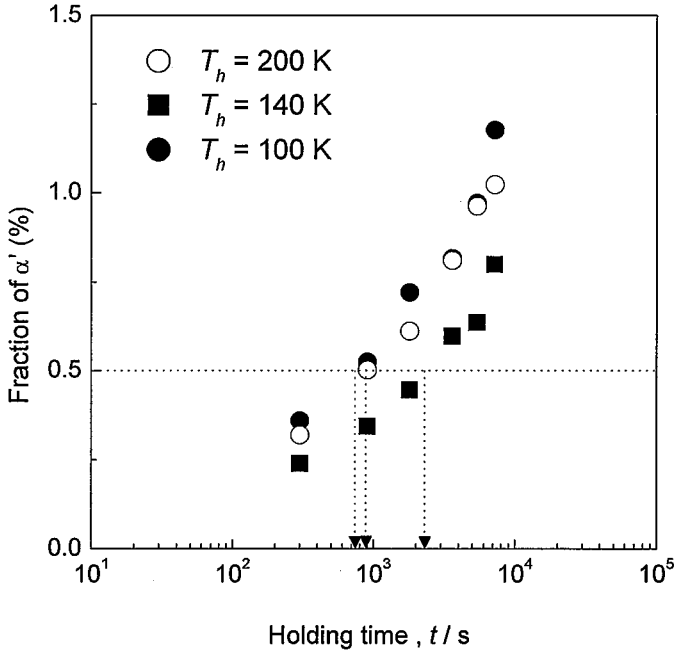

Fig. 4-4 Volume fractions of α'-martensite formed by isothermal holding at 200, 140 and 100 K in the sensitized SUS304 stainless steel. The curve is guide for eyes.

absent of magnetic field at several temperatures in the temperature range between 60 and 260 K, followed by magnetization measurement at room temperature. Figure 4-3 shows typical magnetization curves (*M-H* curves) after isothermal holding experiments of at 200 K. We know from Fig. 4-3 that the magnetization increases with increasing isothermal holding time, meaning that the amount of the ferromagnetic α′-martensite increases by isothermal holding at 200 K. We can evaluate the volume fraction of the α′-martensite by using the value of the spontaneous magnetization, where the value of the spontaneous magnetization is estimated as indicated with an arrow in Fig. 4-3 (g). We notice in Fig. 4-3 (a) that the spontaneous magnetization exists even after isothermal holding for 0 s. This result is probably attributed to the spontaneous magnetization of the carbide $M_{23}C_6$ formed by the sensitization treatment[19]. From the values of spontaneous magnetization, the volume fraction of α′-martensite, $f_{\alpha'}$, can be obtained quantitatively. That is, $f_{\alpha'} = (M_0(T_R) - M_0^{Carbide}(T_R)) / M_0^{\alpha'}(T_R)$, where $M_0(T_R)$ is the spontaneous magnetization at room temperature of the specimen after isothermal holding,

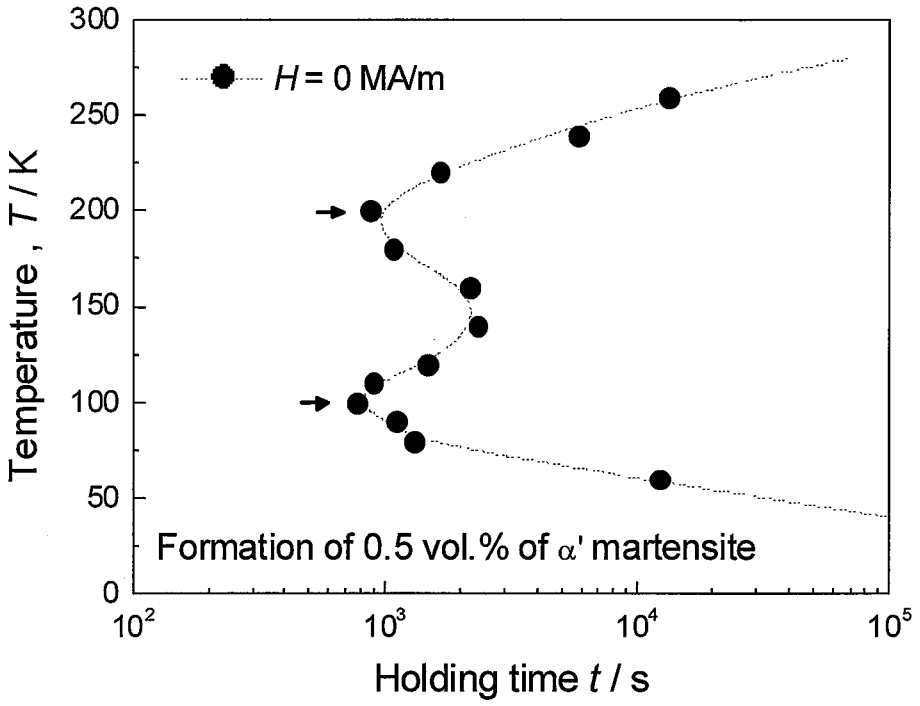

Fig. 4-5 *TTT* diagram of the isothermal martensitic transformation in the sensitized SUS304, and dashed line is guide for eyes.

$M_0^{Carbide}(T_R)$ is that of the as-sensitized specimen, and $M_0^{\alpha'}(T_R)$ is that of the α′-martensite. Here, the value of $M_0^{\alpha'}(T_R)$ can be approximated as the value at 0 K, $M_0^{\alpha'}$(0 K), because the Curie temperature is far above room temperature. Also, $M_0^{\alpha'}$(0 K) is estimated to be 1.79 μ_B/atom considering the Slater-Pauling curve and their valence electron concentration[20]. The volume fraction thus obtained at 200 K is plotted as a function of holding time in Fig. 4-4, together with the results obtained at 140 and 100 K. We know from the result that the $f_{\alpha'}$ obviously depends on isothermal holding temperature as well as isothermal holding time. From the curve in Fig. 4-4, we have constructed the *TTT* diagram of 0.5 vol. % of α′-martensite. The time required for the formation of 0.5 vol. % of α′-martensite is evaluated to be 860, 2320 and 770 s for isothermal holding temperature at 200, 140 and 100 K, respectively. The same experiments have been made in the temperature range between 260 and 60 K, and we have obtained the time required for the formation of 0.5 vol. % of the α′-martensite at these temperatures. Using these times obtained from the evaluation, we have constructed the *TTT* diagram of α′-martensite as shown in Fig. 4-5. It should be noted that the *TTT* diagram shows double C-curve with two noses located at about 100 and 200 K as indicated by arrows. This result is completely different from the *TTT* diagram of the solution-treated SUS304L stainless steel, in which only one nose appears, as shown in chapter 3.

4.3.2. Morphologies of martensites formed during isothermal holding

In order to know the reason why two noses appear in the *TTT* diagram, we have made *in-situ* optical microscope observation during the isothermal holding at the nose temperatures, 100 and 200 K, of the double C-curve. Figures 4-6 and 4-7 show a series of optical micrographs during the isothermal holding at 200 K related to the upper part of the double C-curve. After isothermal holding for 300 s, we can see that wedge-shaped plates, indicated by "A", forms directly in the matrix (γ-phase) in the vicinity of grain boundaries as shown in Fig 4-6 (b). These plates are α′-martensite because the wedge-shaped morphology is characteristic to the α′-martensite[21]. We notice that the number of α′-plates increases near the grain boundaries gradually with increasing the isothermal holding time. In addition, the size of α′-martensite

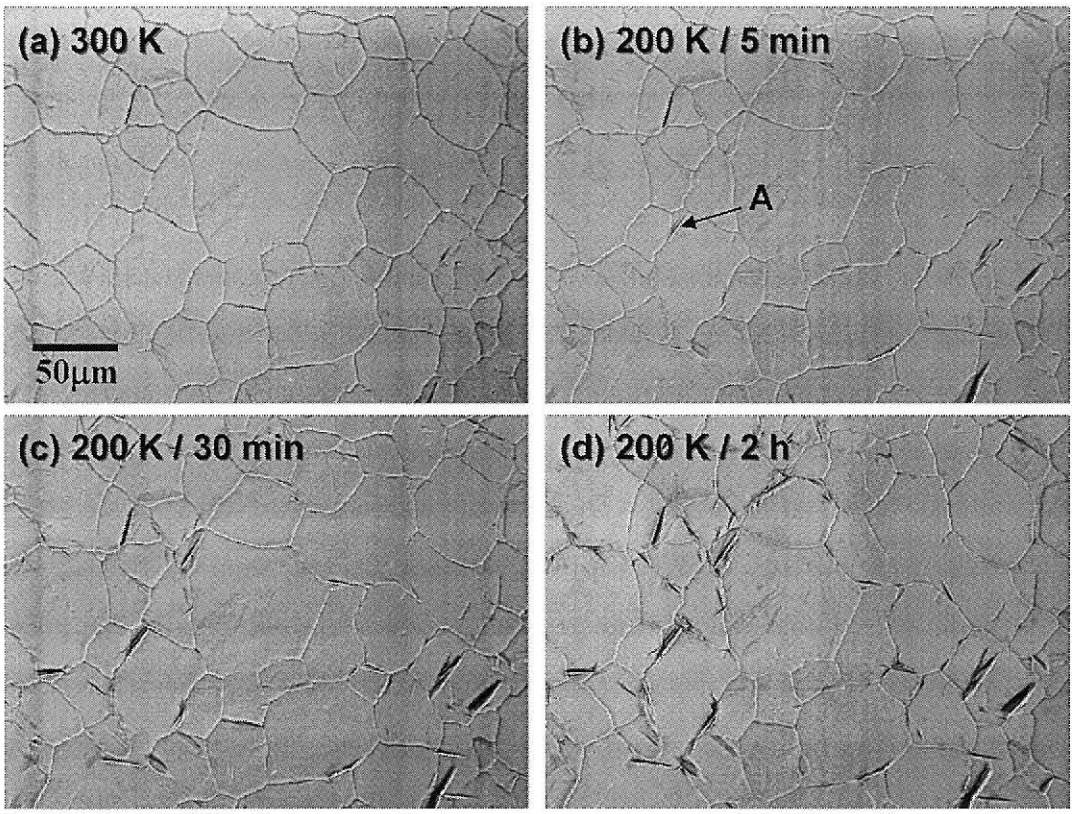

Fig. 4-6 A series of *in-situ* optical micrographs of the sensitized SUS304 stainless steel during isothermal holding at 200 K.

gradually increases with increasing the isothermal holding time. The gradual growth is clearly seen in Fig. 4-7, which is taken from a different region. In the figure, the α′-plate indicated by an arrow obviously grows with increasing holding time. Such a gradual growth of the α′-plate

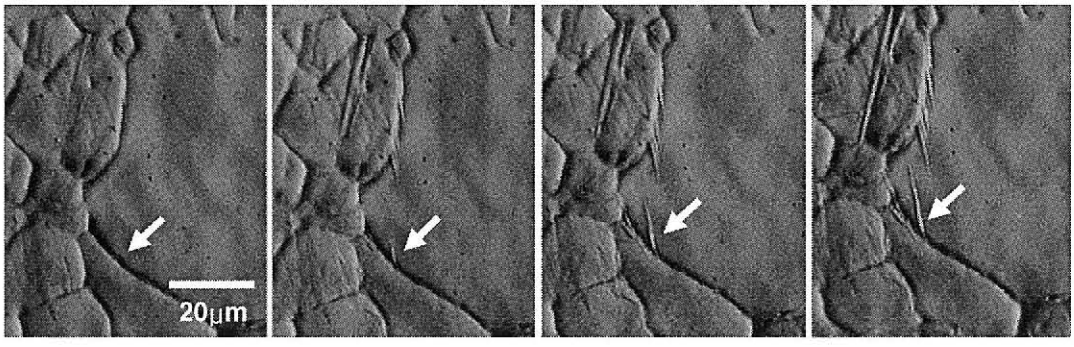

Fig. 4-7 A series of *in-situ* optical micrographs of the sensitized SUS304 stainless steel during isothermal holding at 200 K. Holding times, *t*, at 200 K are inscribed beneath each photograph.

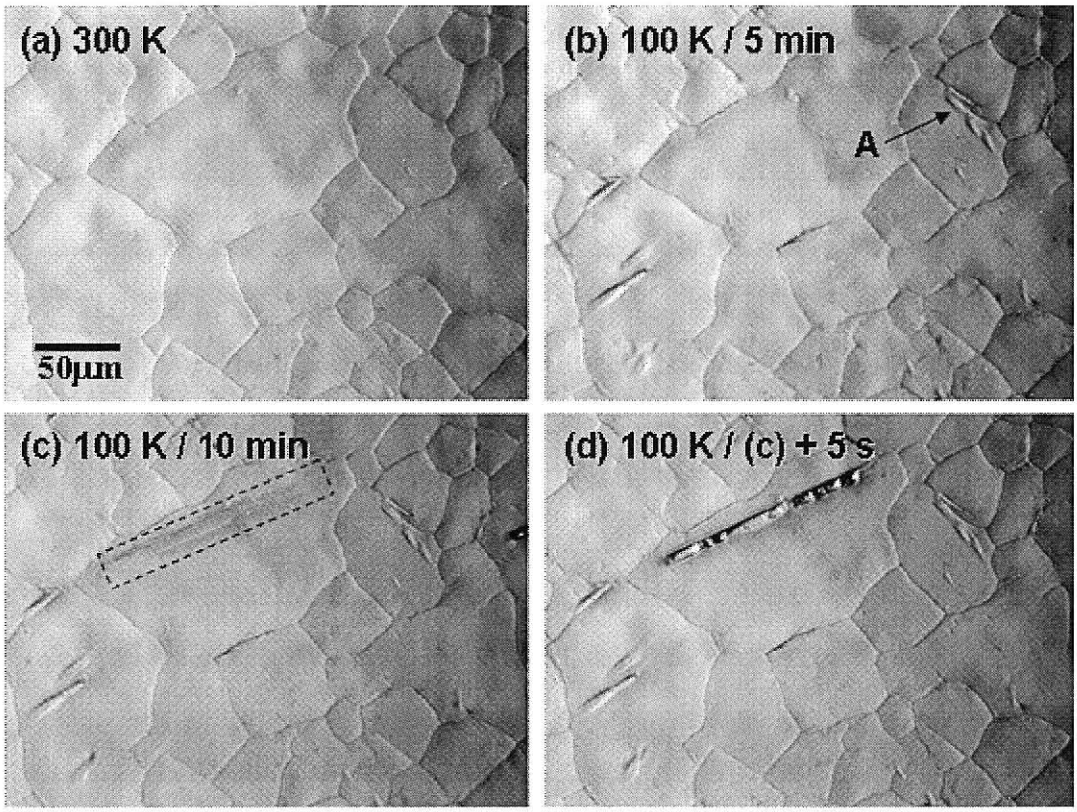

Fig. 4-8 A series of *in-situ* optical micrographs of the sensitized SUS304 stainless steel during isothermal holding at 100 K.

resembles that reported in Fe-Ni-Mn and Fe-Ni-Cr alloys[22-25]. From the above results, we suggest that the upper part of the double C-curve should be related to the direct $\gamma \rightarrow \alpha'$ martensitic transformation induced isothermally in the vicinity of grain boundary during the isothermal holding experiment.

On the other hand, Fig. 4-8 shows a series of optical micrographs taken during the isothermal holding experiment at 100 K, the nose temperature of the lower part of the double C-curve. After isothermal holding for 10 min, a banded plate (characteristic to the ε'-martensite) appears gradually near the center of grains indicated by a dashed rectangle in Fig. 4-8 (c). Similar microstructure has been observed in the solution treated SUS304L after isothermal holding in chapter 3. This result suggests that the $\gamma \rightarrow \varepsilon'$ martensitic transformation proceeds isothermally. Figure 4-8 (d) shows the microstructure taken at the time of 5 sec after observing Fig. 4-8 (c). We notice wedge-shaped plates (α'-martensite) instantaneously formed in the

banded ε′-martensite. That is, the ε′ → α′ martensitic transformation proceeds athermally. In this way, we confirm that the lower part of double C-curve is related to the successive γ → ε′ → α′ martensitic transformation induced near the center of grains during the isothermal holding experiment. Incidentally, we can also observe the α′ martensites formed directly in the vicinity of the grain boundaries after isothermal holding for 5 min in Fig. 4-8 (b), as indicated by "A". This morphology is similar to the result obtained at 200 K. However, the amount of α′ martensites formed directly from grain boundary does not increase on further increasing the isothermal holding time at 100 K. Therefore, it is likely that such direct α′ martensites shown in Fig. 4-8 (b) had been formed at about 200 K during the cooling process.

To understand the martensitic transformation sequence in the sensitized SUS304 stainless

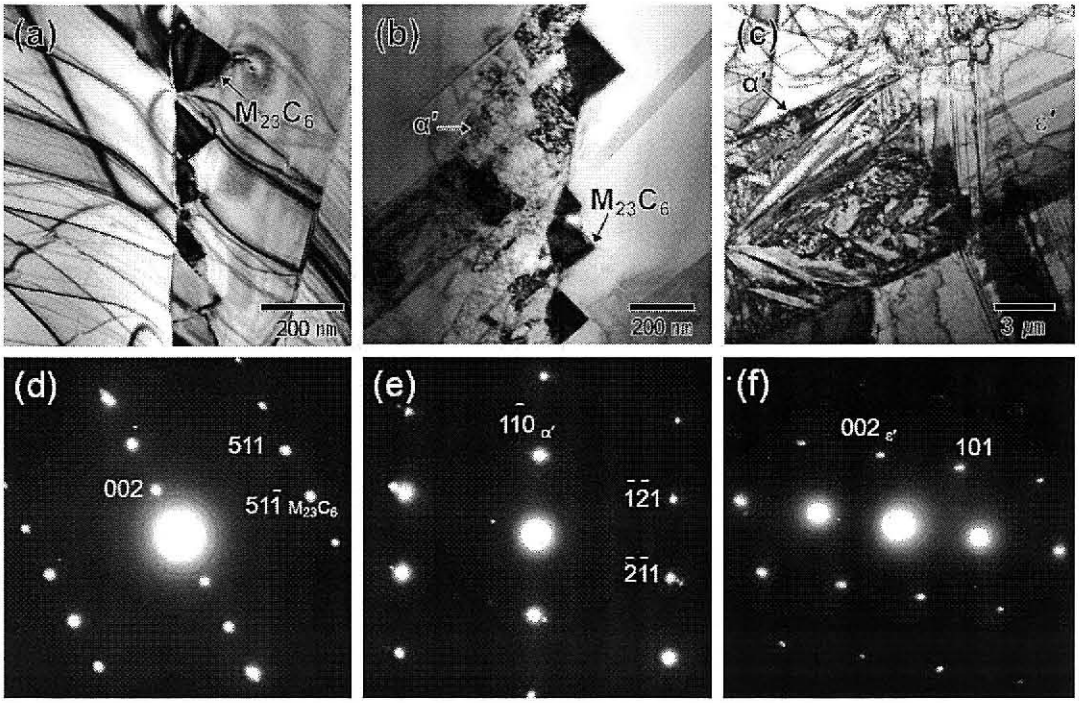

Fig. 4-9 TEM observation results of the sensitized SUS304 stainless steel. (a) is bright field image of the as-sensitized specimen obtained from the vicinity of grain-boundary, (b) is bright field images of the sensitized specimen beforehand isothermal hold at 200 K obtained from the vicinity of grain-boundary, and (c) is bright field image of the sensitized specimen beforehand isothermal holding at 100 K obtained from the center of grain-boundary, respectively. (d), (e) and (f) are electron diffraction patterns corresponding to (a), (b) and (c), respectively.

steel further, the microstructure formed by isothermal holding experiment is examined by using TEM. Figure 4-9 (a) shows a bright field image obtained from the as-sensitized specimen. We can see a grain boundary and some precipitates along the grain boundary. The electron diffraction pattern of these precipitates (Fig. 4-9 (d)) can be indexed with the carbide $M_{23}C_6$, which is formed by sensitization. This result strongly suggests that the chemical composition of the matrix near the grain boundaries should be different from that of the center of grains. Figure 4-9 (b) shows a bright field image after isothermal holding at 200 K. The carbide precipitates are also observed along the grain boundary. In addition, we notice that α'-martensite is formed near the grain boundary, which is known from the electron diffraction pattern corresponding to the encircled area (Fig. 4-9 (e)). This result also confirms that the martensitic transformation sequence on the upper nose of double C-curve is direct $\gamma \rightarrow \alpha'$ martensitic transformation. Figure 4-9 (c) shows the bright field image of the specimen after isothermal holding at 100 K. The image was obtained from the inner region of a grain. We can see that some banded plates of the ε'-phase are formed from γ-phase, and α'-phase is induced inside the banded ε' plates. Such a coexistence with γ-, ε'- and α'-phase suggests that the martensitic transformation sequence corresponding to the lower nose of the double C-curve is successive $\gamma \rightarrow \varepsilon' \rightarrow \alpha'$ martensitic transformation.

4.4 Conclusions

We have investigated *TTT* diagram of isothermal martensitic transformation in a sensitized SUS304 stainless steel and the following results have been obtained.

(1) Sensitized SUS304 stainless steel exhibits an isothermal martensitic transformation when the specimen is held in the temperature range between 60 and 260 K.

(2) *TTT* diagram of the martensitic transformation shows a double-C curve with two noses

located at about 100 and 200 K due to two different transformation sequences: the upper and lower parts of the double C-curve are ascribed to the direct $\gamma \rightarrow \alpha'$ martensitic transformation in the vicinity of grain boundaries and the successive $\gamma \rightarrow \varepsilon' \rightarrow \alpha'$ martensitic transformation near the center of grains, respectively.

Reference

[1] D. C. Larbalestier and H.W. King, *Cryogenics* **13** (1973) 160

[2] D. T. Read and R. P. Reed, *Cryogenics* **21** (1981) 415

[3] T. Tanaka, T. Kadota, Y. Kohno and K. Shibata, *Adv. Cryogenic Engng. Mater.* **44** (1998) 1

[4] J. W. Chan, D. Chu, A. J. Sunwoo and J. W. Morris, Jr., *Adv. Cryogenic Engng. Mater.* **38** (1992) 55

[5] S. Murase, S. Kobatake, M. Tanaka, I. Tashiro, O. Horigami, H. Ogiwara, K. Shibata, K. Nagai and K. Ishikawa, *Fusion Eng. Des.* **20** (1993) 451

[6] N. Yasumaru, *Mater. Trans.* **39** (1998) 1046

[7] K. Mumtaz, S. Takahashi, J. Echigoya, L. F. Zhang, Y. Kamada and M. Sato, *J. Mater. Sci.* **38** (2003) 3037

[8] E. Nagy, V. Mertinger, F. Tranta and J. Sólyom, *Mater. Sci. Eng. A* **378** (2004) 308

[9] K. Mumtaz, S. Takahashi, J. Echigoya, Y. Kamada, L. F. Zhang, H. Kikuchi, K. Ara and M. Sato, *J. Mater. Sci.* **39** (2004) 1997

[10] L. Zhang, S. Takahashi, Y. Kamada, H. Kikuchi, K. Ara, M. Sato and T. Tsukada, *J. Mater. Sci.* **40** (2005) 2709

[11] Y. Kamada, T. Mikami, S. Takahashi, H. Kikuchi, S. Kobayashi and K. Ara, *J. Magn. Magn. Mater.* **310** (2007) 2856

[12] A. Miller, Y. Estrin and X. Z. Hu, *Scripta Mater* **47** (2002) 441

[13] A. Mitra, P. K. Srivastava, P. K. De, D. K. Bhattacharya and D. C. Jiles, *Metall. Mater. Trans. A* **35A** (2004) 559

[14] F. De Backer, V. Schoss and G. Maussner, *Nucl. Eng. Des.* **206** (2001) 201

[15] R. G. BAKER and J. NUITING, *J. Iron Steel Inst.* **192** (1959) 257

[16] S.M. Bruemmer and L.A. Charlot, *Scr. Metall.* **20** (1986) 1019

[17] N. Parvathavarthini and R.K. Dayal, *J. of Nuclear Materials* **305** (2002) 209

[18] V. Kain, R.C. Prasad, P.K. De, Corrosion 58 (2002) 15.

[19] J. Szczytko, P. Osewski, M. Bystrzejewski, J. Borysiuk, A. Grabias, A. Huczko, H. Lange,

A. Majhofer and A. Twardowski: Acta Phy. Pol. **112** (2007) 305-310.

[20] J. Crangle and G. C. Hallam, *Proc. Poy. Soc.* **A272** (1963) 119

[21] A. K. De, D. C. Murdock, M. C. Mataya, J. G. Speer and D. K. Matlock, *Scr. Mater.* **50** (2004) 1445

[22] T. Kakeshita, Y. Sato, T. Saburi, K. Shimizu, Y. Matsuoka, K. Kindo and S. Endo, *Trans. JIM* 40 (1999) 107

[23] T. Kakeshita, K. Kuroiwa, K. Shimizu, T. Ikeda, A. Yamagishi and M. Date, *Trans. JIM* **34** (1993) 423

[24] T. Kakeshita, K. Kuroiwa, K. Shimizu, T. Ikeda, A. Yamagishi and M. Date, *Trans. JIM* **34** (1993) 415

[25] T. Kakeshita, Y. Sato, T. Saburi, K. Shimizu, Y. Matsuoka and K. Kindo, *Trans. JIM* **40** (1999) 100

Chapter 5

Effect of magnetic field on the C-curve of successive $\gamma \rightarrow \varepsilon' \rightarrow \alpha'$ martensitic transformation in solution-treated SUS304L stainless steel

5.1 Introduction

In chapter 2 and 3, we found successive $\gamma \rightarrow \varepsilon' \rightarrow \alpha'$ martensitic transformation in solution-treated SUS304L stainless steel during the isothermal holding in the temperature range between 70 K and 170 K, and then we constructed *TTT* diagram of successive $\gamma \rightarrow \varepsilon' \rightarrow \alpha'$ martensitic transformation, in which *TTT* diagram shows a C-curve with a nose temperature located at about 103 K. Optical microscope observation suggests that the $\varepsilon' \rightarrow \alpha'$ transformation proceeds athermally while the $\gamma \rightarrow \varepsilon'$ transformation proceeds isothermally. However, the kinetics of successive $\gamma \rightarrow \varepsilon' \rightarrow \alpha'$ martensitic transformation is not clear yet. Kakeshita *et al.* proposed that kinetics of martensitic transformation can be understood by measuring the effect of magnetic field on the transformation[1-2], as mentioned section 1.3.3.

In this chapter, therefore, we investigate the effect of magnetic field on successive $\gamma \rightarrow \varepsilon' \rightarrow \alpha'$ martensitic transformation in solution-treated SUS304L in order to obtain information about kinetics of the martensitic transformation. Furthermore, we calculate the effect of magnetic field on martensitic transformation by using a phenomenological theory mentioned in the appendix of this chapter. Finally, we compare the calculated relations with the experimentally measured ones

5.2 Experimental Procedure

The chemical composition of SUS304L stainless steel used in this chapter is the same as that shown in Table 2-1. Specimens of 3 × 3 × 1 mm in size were cut out from a cold-rolled sheet, and were solution-treated at 1323 K for 0.5 h in vacuum followed by quenching into iced water. Then the oxidized surface layer was eliminated by electropolishing in an electrolyte composed of 85 % C_2H_5OH and 15 % $HClO_4$ in volume.

Isothermal holding experiments of the specimens were carried out under the static magnetic field of 0.8, 4.0 and 5.6 MA/m in the temperature range between 170 and 70 K for various times. The volume fraction of the α′-martensite, $f_{\alpha'}$, formed by the isothermal holding was evaluated by a magnetization measurement at 300 K (= T_R). After isothermal holding experiment, the microstructure was investigated by optical microscopy. Details of experimental procedure were described in chapter 2.

5.3 Results

5.3.1 Effect of magnetic field on C-curve

In order to investigate the variation of C-curve under magnetic field, we have made isothermal holding experiment under magnetic fields of 0.8, 4.0 and 5.6 MA/m in the temperature range between 170 and 70 K, followed by magnetization measurement at room temperature. Figure 5-1 shows typical magnetization curves after isothermal holding experiments at 103 K under the magnetic field of 0.8 MA/m. We know from Fig. 5-1 that the magnetization increases with increasing isothermal holding time, meaning that the amount of the ferromagnetic α′-martensite increases by isothermal holding at 103 K. Such increase of magnetization by increasing isothermal holding time was also observed under magnetic fields of 4.0 and 5.6 MA/m. We can evaluate the volume fraction of the α′-martensite by using the value of the spontaneous magnetization, as described in chapter 3. The relation between

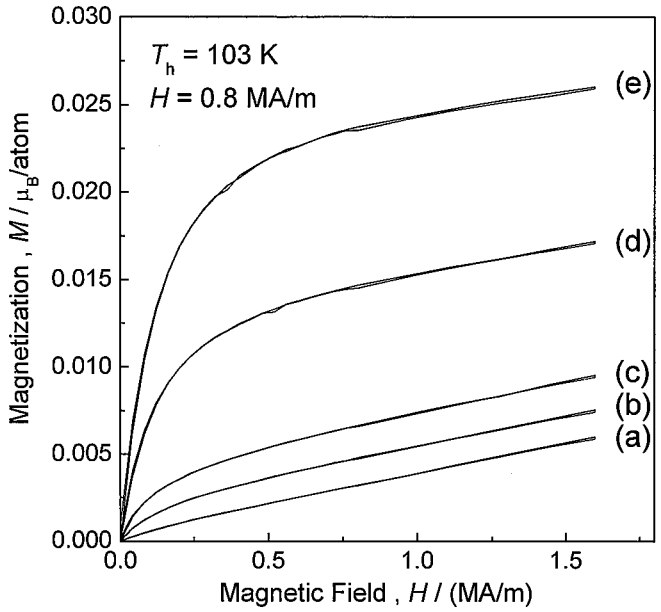

Fig. 5-1 Magnetization curves obtained at 300 K for the solution-treated SUS304L stainless steel after isothermal holding at 103 K for 70 s (a), 210 s (b), 760 s (c), 1680 s (d) and 4860 s (e), respectively, under magnetic field of 0.8 MA/m.

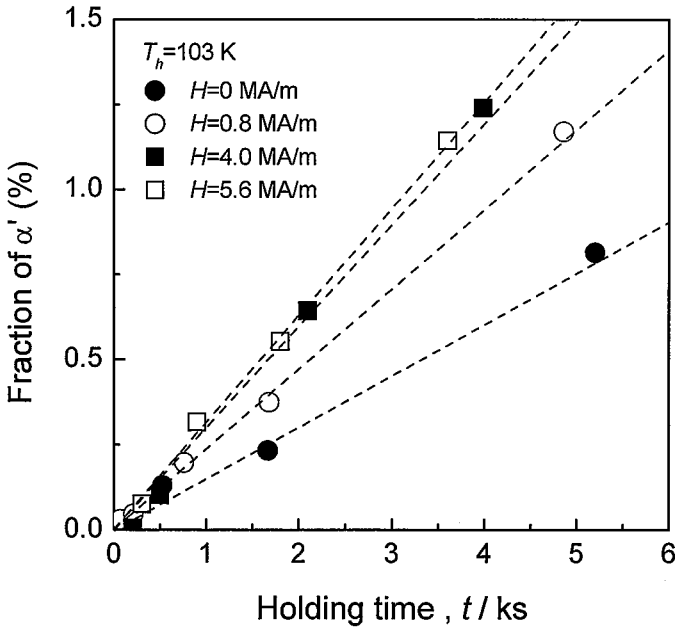

Fig. 5-2 Relation between isothermal holding time and volume fraction of α′-martensite in the solution-treated SUS304L after isothermal holding at 103 K under various magnetic fields of 0, 0.8, 4.0, and 5.6 MA/m. Lines are guide for eyes.

isothermal holding time and volume fraction of the α′-martensite after isothermal holding at 103 K thus obtained are shown with open circles (0.8 MA/m), solid squares (4.0 MA/m) and open squares (5.6 MA/m) in Fig. 5-2. In the figure, the relation under no magnetic field is also shown with solid circles (0 MA/m). We know from the result that the $f_{\alpha'}$ obviously depends on the strength of magnetic field as well as isothermal holding time. From the lines in Fig. 5-2, we have constructed the C-curve of 0.5 vol. % of α′-martensite. The time required for the formation of 0.5 vol. % of α′-martensite at 103 K is evaluated to be 6080, 3500, 3000 and 2800 s for strength of magnetic field of 0, 0.8, 4.0 and 5.6 MA/m, respectively. The same experiments have been made in the temperature range between 170 and 70 K under various magnetic fields, and we have obtained the time required for the formation of 0.5 vol. % of α′-martensite. Using these times, we have confirmed the variation of C-curves. Fig. 5-3 shows variation of C-curves related to the α′-martensite formed by 0.5 % in solution-treated SUS304L stainless steel under the magnetic field of 0 MA/m (solid circles), 0.8 MA/m (open circles), 4.0

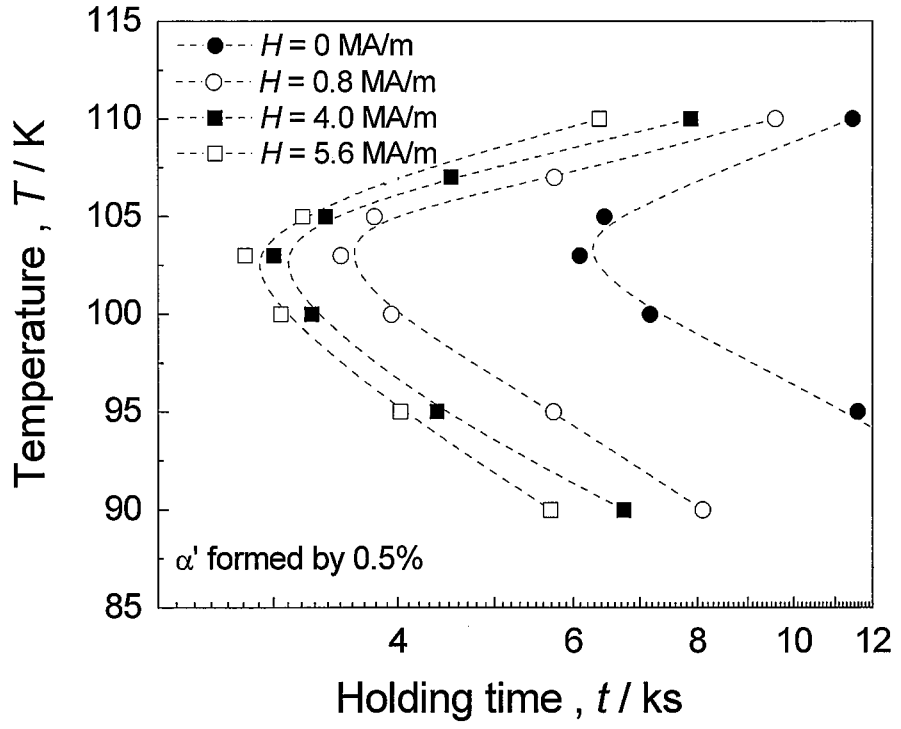

Fig. 5-3 Variation of C-curves related to α′-martensite formed by 0.5 % in the solution-treated SUS304L stainless steel under magnetic fields. Dashed lines are guide for eyes.

MA/m (solid squares) and 5.6 MA/m (open squares) in solution-treated SUS304L stainless steel. It should be noted in Fig. 5-3 that the nose temperatures of C-curves are located at about 103 K under all magnetic fields, and C-curves shift to the side for a short time with increasing the strength of magnetic field. This result is different from that of Fe-Ni-Cr and Fe-Ni-Mn alloys exhibiting isothermal $\gamma \rightarrow \alpha'$ martensitic transformation, whose incubation time shortens and nose temperature decreases with increasing the strength of magnetic field [3-6]. There is another difference in the magnetic field dependence of C-curve. That is, the shift in C-curve is small for high magnetic field region in the present SUS304L steel, while not in Fe-Ni-Cr and Fe-Ni-Mn alloys. This difference should be ascribed to the difference in kinetics of martensitic transformation between them, which will be discussed later.

Incidentally, we notice that the shape of the C-curve changes by the application of magnetic field. That is, the decrease in holding time below the nose temperature is larger than that above the nose temperature. This difference is possibly attributed to the temperature dependence of the spontaneous magnetization of α'-martensite.

5.3.2 Morphologies of martensites formed during isothermal holding

Figure 5-4 shows optical micrographs of thermally-induced martensites by isothermal

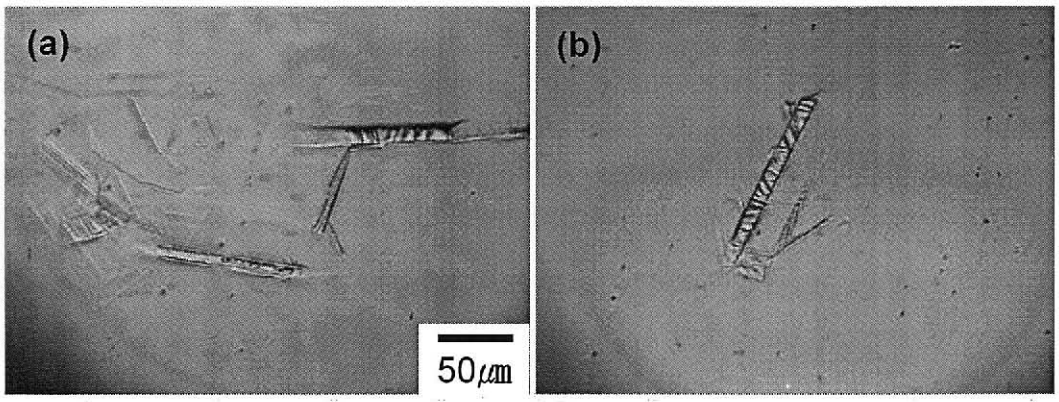

Fig. 5-4 Optical micrographs of martensites formed by isothermal holding at 103 K for 10 min under zero magnetic field (a), and for 5 min under magnetic field of 5.6 MA/m. Observations were made at room temperature after isothermal holding experiments.

holding at 103 K. (a) is obtained in the absence of magnetic field (H = 0 MA/m) and (b) is obtained under applied magnetic field of H = 5.6 MA/m, where the isothermal holding experiments are carried out for different period in order to form the same amount of α′-martensite. It should be noted from the result that the amount of α′-martensites is almost the same in both specimens, while the amount of ε′-martensites decreases with increasing the strength of applied magnetic field. This means that the α′-martensites form more easily from the ε′-martensite with increasing strength of the magnetic field. Incidentally, the morphology of thermally-induced α′-martensites does not depend on the strength of applied magnetic field. The effect of magnetic field on morphology of martensites formed during isothermal holding will be also discussed later.

5.4 Discussion

Based on the results obtained in the results of this chapter and chapter 3, we discuss the kinetics of successive γ → ε′ → α′ martensitic transformation in solution-treated SUS304L stainless steel.

Before discussing effect of magnetic field, we discuss the transformation behavior under no magnetic field. In chapter 3, we suggested from the morphology changes under no magnetic field that the successive γ → ε′ → α′ martensitic transformation is divided into isothermal γ → ε′ martensitic transformation and athermal ε′ → α′ martensitic transformation. Morphology of each phase on *TTT* diagram under no magnetic fields is estimated from the observation and is schematically shown in Fig. 5-5. In this figure, we assumed that the sizes of ε′- and α′-martensites are the same on the C-curve. We suggest in this figure that α′-martensite instantaneously forms from ε′-martensites when a banded ε′-martensite becomes a certain size, and the amount of α′-martensite increases with increasing the amount of such ε′-martensites at the same temperature ($T = T_1$).

If we assume that the amount of ε′-martensite is the same on the *TTT* diagram as discussed

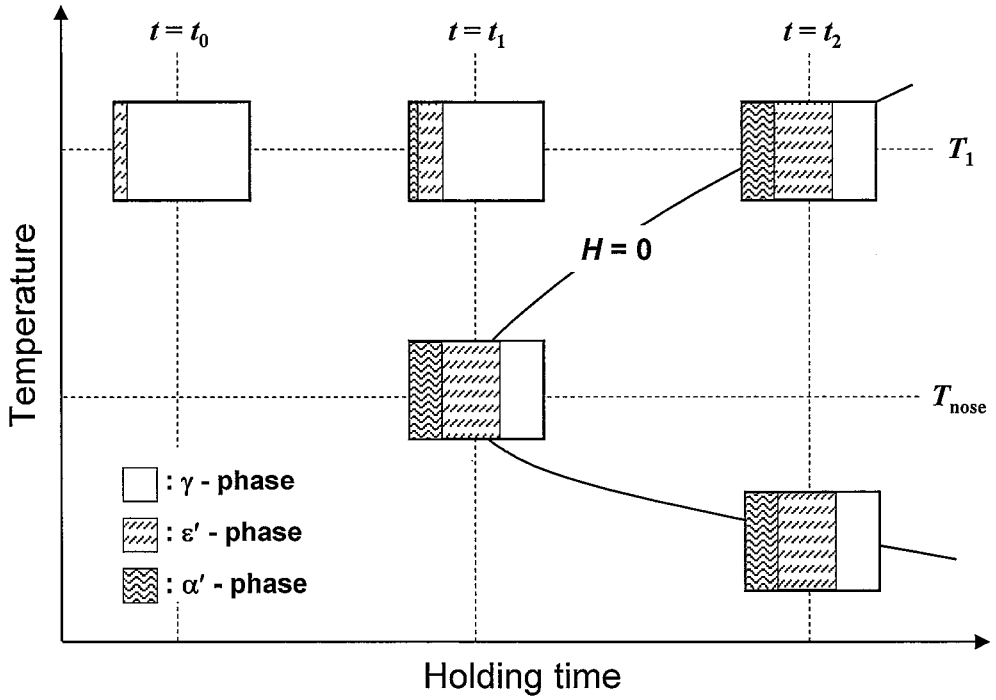

Fig. 5-5 Schematic illustration showing the morphology of martensite on *TTT* diagrams under no magnetic field.

above, we know the chemical free energy difference between ε′- and γ-phases of SUS304L stainless steel by using the phenomenological theory proposed by Kakeshita *et al.* According to the phenomenological theory (Appendix), the transition probability P_e of the $\gamma \rightarrow \varepsilon'$ martensitic transformation can be expressed as

$$P_e = P_0 \cdot \exp\left(-\Delta_{\gamma \rightarrow \varepsilon'} / k_B T\right) \qquad (5\text{-}1)$$

where $\Delta_{\gamma \rightarrow \varepsilon'}$ is the potential barrier (activation energy) for the $\gamma \rightarrow \varepsilon'$ transformation. The value of $\Delta_{\gamma \rightarrow \varepsilon'}$ is related to the free energy difference between γ- and ε′-phases $\Delta G^{\gamma \rightarrow \varepsilon'}(T)$, as described in the Appendix. The experimentally obtained C-curve under no magnetic field is well fitted by using the following $\Delta G^{\gamma \rightarrow \varepsilon'}(T)$

$$\Delta G^{\gamma \rightarrow \varepsilon'}(T) = 100 - [0.12 \times \exp((T - 5) / 11.937)] \text{ J/mol} \qquad (5\text{-}2)$$

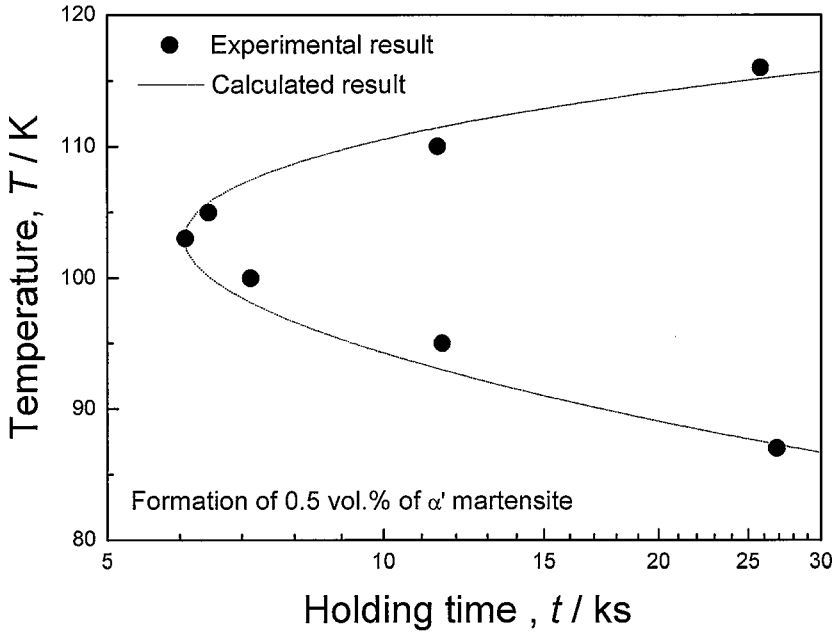

Fig. 5-6 *TTT* diagram of the isothermal martensitic transformation in the solution-treated SUS304L stainless steel under no magnetic field, and dotted line is the calculated relations.

This value of $\Delta G^{\gamma \rightarrow \varepsilon'}(T)$ evaluated from above relation is the same order with experimental result reported so far for fcc → bcc transformation[7-8]. The calculated *TTT* diagram obtained using eq. (5-1) and $\Delta G^{\gamma \rightarrow \varepsilon'}(T)$ of eq. (5-2) is shown by a dotted curve in Fig 5-6. It reproduces experimental result, meaning that above assumption (the amount of ε′-martensite is same on *TTT* diagram) is appropriate.

Now we are ready to discuss the effect of magnetic field on the C-curve for successive γ → ε′ → α′ transformation.

In Fig. 5-3, we observed that the nose temperature does not depend on the strength of magnetic field. We first discuss the reason. As mentioned above, only the γ → ε′ martensitic transformation proceeds isothermally in solution-treated SUS304L stainless steel, and the ε′ → α′ transformation proceeds athermally. Therefore, the nose temperature of C-curve should be related to isothermal γ → ε′ martensitic transformation only. From eq. (5-1), it is clear that the transition probability, P_e, of the γ → ε′ martensitic transformation depend on $\Delta_{\gamma \rightarrow \varepsilon'}$, the activation energy for the γ → ε′ transformation. In the γ → ε′ martensitic transformation,

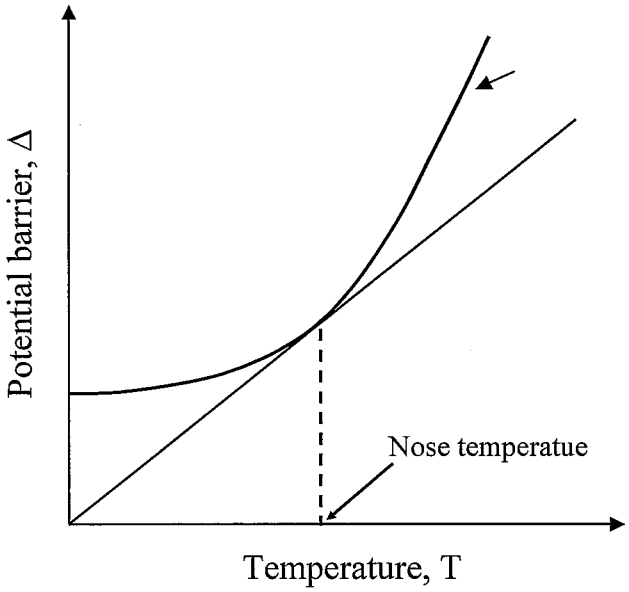

Fig. 5-7 Schematic diagram of relation between potential barrier ($\gamma \rightarrow \varepsilon'$) and temperature.

however, $\Delta_{\gamma \rightarrow \varepsilon'}$ does not change by the application of magnetic field because γ-phase and ε′-martensite of solution-treated SUS304L have non-magnetic properties in the temperature range exhibiting isothermal martensitic transformation. Therefore, the $\gamma \rightarrow \varepsilon'$ martensitic transformation could not be influenced by the application of magnetic field, and the nose temperature of C-curve also does not change as shown in Fig 5-7.

Next, we discuss the reason why the C-curve, corresponding to the formation of 0.5% α′-martensite, shifts by the application of magnetic field in the present SUS304L steel. As described above and in chapter 3, the isothermal nature should be due to the $\gamma \rightarrow \varepsilon'$ transformation, and the $\varepsilon' \rightarrow \alpha'$ transformation will occur instantaneously when ε′-plate grows to a critical size. We also found in chapter 2 that the magnetic field induced $\varepsilon' \rightarrow \alpha'$ transformation occurs in a wide ε′-martensite plate formed by isothermal holding, while not in a thin ε′-martensite plate formed by deformation. Moreover, we observed in Fig. 5-4 that the amount of ε′-martensite is small when α′-martensite is formed under magnetic field compared with that formed without applying magnetic field. Form these results, we are confident that α′-martensite can be formed from smaller ε′-martensite when magnetic field is applied. Incidentally, ε′-martensite grows with increasing time for its isothermal nature. In this way,

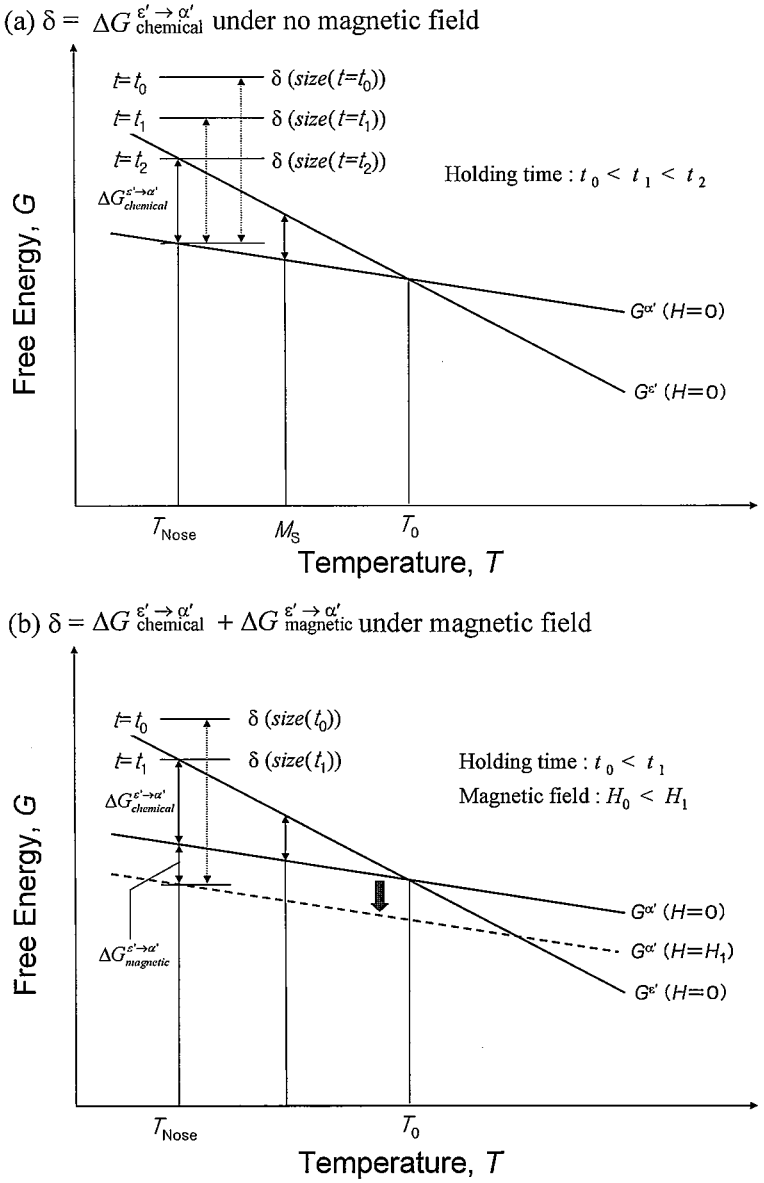

Fig. 5-8 Schematic diagrams for variation of ε′ → α′ martensitic transformation under no magnetic field (a), and under magnetic field (b).

the time required for the formation of α′-martensite should shorten by the application of magnetic field.

Then the problem is to clarify the reason why the α′-martensite can be formed form smaller ε′-martensite by the application of magnetic field. We discuss this behavior by considering driving force of the ε′ → α′ transformation. Since the ε′ → α′ transformation

depends on the size of ε′-martensite, which grows with increasing time, we may assume that the driving force, δ, for the ε′ → α′ transformation decreases with increasing the size of ε′-martensite, i.e., with increasing holding time. Figure 5-8 (a) shows the holding time dependence of chemical free energy difference $\Delta G_{chemical}^{\varepsilon'\rightarrow\alpha'}$ and δ (*size*). The driving force δ (*size*) will decrease with increasing holding time because of the decrease in elastic energy per volume, and it becomes $\Delta G_{chemical}^{\varepsilon'\rightarrow\alpha'}$ at holding time t_2, at which the α′-martensite forms in the ε′-martensite. If a magnetic filed of H_1 is applied, magnetic energy difference $\Delta G_{magnetic}^{\varepsilon'\rightarrow\alpha'}$ arises between ε′- and α′-phase, and it fills a part of driving force as shown in Figure 5-8 (b) in addition to $\Delta G_{chemical}^{\varepsilon'\rightarrow\alpha'}$. Then the transformation occurs at a shorter holding time t_1. This means that α′-martensite can be induced from a smaller size of thermally-induced ε′-martensite under a magnetic field. The effect of such holding time and magnetic field on the morphology change is schematically shown in Fig. 5-9. This schematic illustration is in good agreement with experimental result shown in Fig. 5-3.

Finally, we will roughly estimate how the driving force δ (*size*) changes with increasing holding time at nose temperature (103 K). First, we assume that δ (*size*) at 103K after holding for period t_2 under no magnetic field is 2183 J/mol. This value is determined from $\Delta G_{chemical}^{\varepsilon'\rightarrow\alpha'}$

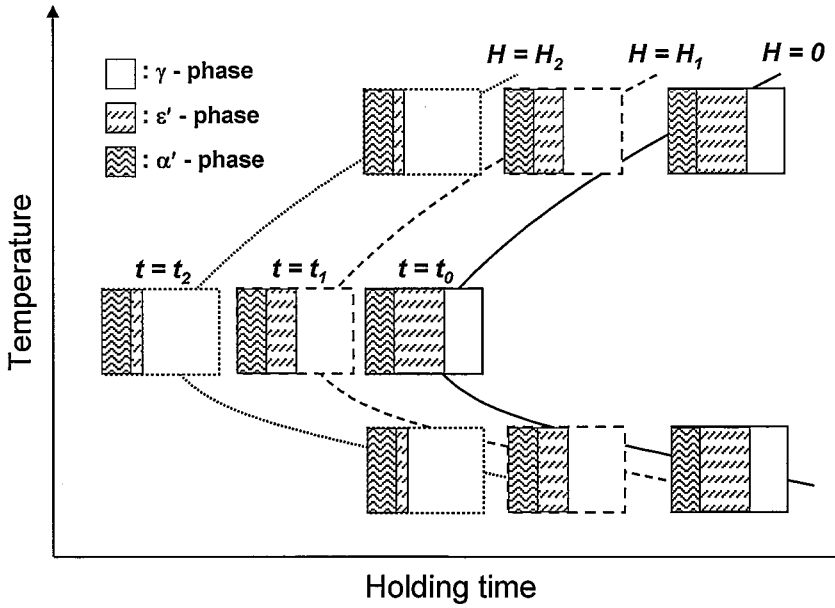

Fig. 5-9 Schematic illustration showing the morphology of martensite on C-curves under various magnetic fields.

of Fe-Ni alloy reported by Kaufman *et al.*[9], because we have no experimental data for the present SUS304L stainless steel. The value of δ (*size*) should be the sum of $\Delta G^{\varepsilon'\rightarrow\alpha'}_{chemical}$ and $\Delta G^{\varepsilon'\rightarrow\alpha'}_{magnetic}$ at the initiation time for the ε′ → α′ transformation. Thus the following relation should be satisfied on the C-curve, on which the ε′ → α′ transformation initiates.

$$\delta\,(size) = \Delta G^{\varepsilon'\rightarrow\alpha'}_{chemical} + \Delta G^{\varepsilon'\rightarrow\alpha'}_{magnetic} \qquad (5\text{-}3)$$

The value of $\Delta G^{\varepsilon'\rightarrow\alpha'}_{magnetic}$ can be easily calculated by using

$$\Delta G^{\varepsilon'\rightarrow\alpha'}_{magnetic} = M\,(\text{magnetization}) \times H\,(\text{magnetic field}) \qquad (5\text{-}4)$$

where the M is the value of $M_0^{\alpha'}(0)$ of SUS304L stainless steel, and it is estimated to be 1.79 μ_B/atom considering the Slater-Pauling curve and their valence electron concentration[10], as mentioned in chapter 2. H is the strength of magnetic fields applied during the isothermal

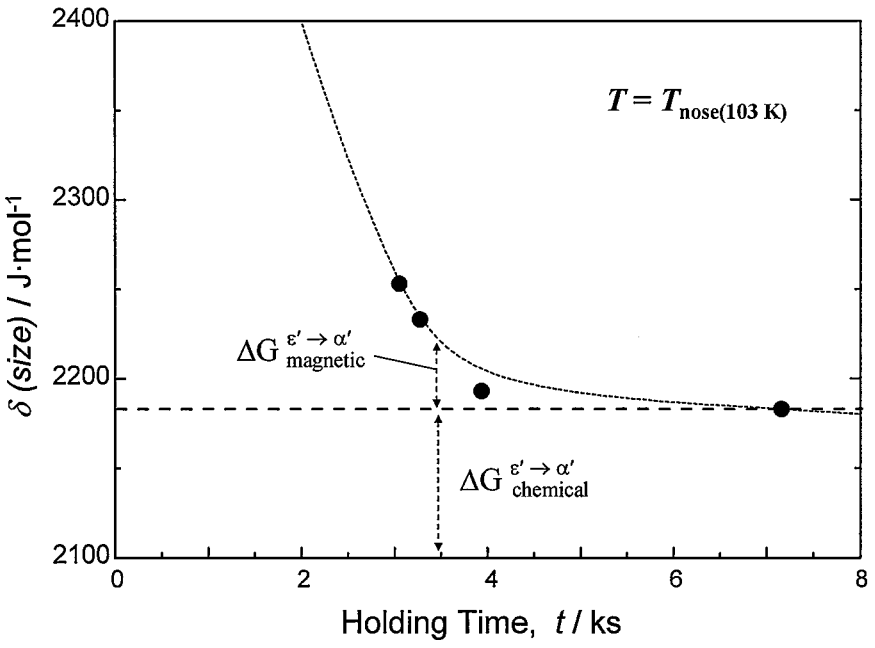

Fig. 5-10 Relation between δ (*size*) and holding time at 103 K in solution-treated SUS304L stainless steel.

holding. Then from the magnetic field dependence of the C-curve, we can obtain time dependence of δ (*size*), which is shown in Figure 5-10. In the figure, the horizontal axis is time instead of size of the ε′-martensite because we do not know exactly the size. However, considering that size of ε′-martensite is a function of time and temperature, such plot should give effective information about how the driving force δ depends on holding time. We know from Figure 5-10 that, δ (*size*) decreases sharply in a short isothermal holding time, and then decreases gradually. This result suggests that, the driving force is very high in thin plate of ε′-martensite, being in good agreement with the results of chapter 2 that magnetic field-induce ε′ → α′ transformation does not occur form thin plate of ε′-martensite formed by deformation induced martensite.

5.5 Conclusions

We have investigated the effect of magnetic field on C-curve of the successive γ → ε′ → α′ martensitic transformation in a solution-treated SUS304L stainless steel and the following results have been obtained.

(1) Nose temperatures of C-curves do not depend on magnetic field strength, it is located at about 103 K for all the magnetic fields examined. This is due to the fact that the γ → ε′ martensitic transformation, having no concern with magnetic field, proceeds isothermally while the ε′ → α′ martensitic transformation, influenced by magnetic field, proceeds athermally.

(2) C-curves shift to the side for a short time with increasing the strength of magnetic field because the magnetic energy difference between the ε′- and α′-phases provides a part of driving force, which is necessary for field-induces ε′ → α′ martensitic transformation.

Reference

[1] T. Kakeshita, T. Yamamoto, K. Shimizu, K. Sugiyama and S. Endo, *Trans. JIM* **36** (1995) 1018

[2] T. Kakeshita, T. Saburi and K. Shimizu, *Marls. Sci. and Eng. A* **273-275** (1999) 21

[3] T. Kakeshita, Y. Sato, T. Saburi, K. Shimizu, Y. Matsuoka, K. Kindo and S. Endo, *Trans. JIM* **40** (1999) 107

[4] T. Kakeshita, K. Kuroiwa, K. Shimizu, T. Ikeda, A. Yamagishi and M. Date, *Trans. JIM* **34** (1993) 423

[5] T. Kakeshita, K. Kuroiwa, K. Shimizu, T. Ikeda, A. Yamagishi and M. Date, *Trans. JIM* **34** (1993) 415

[6] T. Kakeshita, Y. Sato, T. Saburi, K. Shimizu, Y. Matsuoka and K. Kindo, *Trans. JIM* 40 (1999) 100

[7] A. Forsberg, J. Ågren, *J. Phase Equilib.* **14** (1993) 354

[8] M. Palumbo, *Computer Coupling of Phase Diagrams and Thermochemistry* **32** (2008) 693

[9] L. Kaufman, referred to Doctor Thesis by M. K. Korenko, MIT, Cambridge, USA, 1973, P. 72

[10] J. Crangle and G. C. Hallam, *Proc. Poy. Soc.* **A272** (1963) 119

Chapter 6

Summary

In the present study, the effects of cryogenic temperature, high magnetic field, high stress and their combined environments on solution-treated and sensitized austenitic stainless steels (SUS304, SUS304L, SUS316 and SUS316L) have been investigated as a fundamental research to clarify the stability of austenite phase. As a result, the following conclusions have been derived.

In chapter 1, we have introduced the background of present study, followed by the purpose and significance of present study.

In chapter 2, we have examined effects of cryogenic temperature, high stress, high magnetic field and their combined condition on martensitic transformation in SUS304, SUS304L, SUS316 and SUS316L austenitic stainless steels. No athermal martensitic transformation occurs in all the solution-treated and sensitized stainless steels, however, isothermal transformation occurs in the sensitized SUS304 ($\gamma \rightarrow \varepsilon' \rightarrow \alpha'$ and $\gamma \rightarrow \alpha'$) between about 150 K and 250 K. It also occurs in the solution-treated ($\gamma \rightarrow \varepsilon' \rightarrow \alpha'$) and sensitized SUS304L ($\gamma \rightarrow \varepsilon' \rightarrow \alpha'$ and $\gamma \rightarrow \alpha'$) between about 70 and 170 K. Incidentally, the γ-phase in all the steels exhibits an antiferromagnetic transition at about 40 K. Magnetic field-induced martensite transformation does not occur in the γ-phase even when the pulsed magnetic field of up to 30 MA/m is applied in the temperature range between 4.2 and 290 K in all the solution-treated and sensitized stainless steels. On the other hand, deformation-induced $\gamma \rightarrow \varepsilon' \rightarrow \alpha'$ martensite transformation occurs at 77 K for all the solution-treated and sensitized stainless steels. It is noted for the solution-treated SUS304L, sensitized SUS304 and SUS304L stainless steels that magnetic field-induced martensitic transformation ($\varepsilon' \rightarrow \alpha'$) occurs in isothermally

transformed ε′-martensites, but not in deformation-induced ε′-martensites.

In chapter 3, we have constructed time-temperature-transformation (*TTT*) diagram of isothermal martensitic transformation in a solution-treated SUS304L stainless steel, and we found that the *TTT* diagram shows a C-curve with a nose temperature located at about 103 K. The successive $\gamma \rightarrow \varepsilon' \rightarrow \alpha'$ martensitic transformation proceeds by isothermal $\gamma \rightarrow \varepsilon'$ martensitic transformation followed by athermal $\varepsilon' \rightarrow \alpha'$ martensitic transformation.

In chapter 4, we have constructed *TTT* diagram of isothermal martensitic transformation in a sensitized SUS304 stainless steel, and we found that the sensitized specimen exhibits an isothermal martensitic transformation when the specimen is held in the temperature range between 60 and 260 K. The *TTT* diagram corresponding to the formation of 0.5 vol. % of α′-martensite shows a double-C curve with two noses located at about 100 and 200 K. An *in-situ* optical microscope observation has revealed that the double C-curve is due to two different transformation sequences. That is, the upper part of the C-curve is attributed to the direct $\gamma \rightarrow \alpha'$ martensitic transformation and the lower part of the C-curve is due to the successive $\gamma \rightarrow \varepsilon' \rightarrow \alpha'$ martensitic transformation. The direct $\gamma \rightarrow \alpha'$ transformation occurs in the vicinity of grain boundaries, while the successive $\gamma \rightarrow \varepsilon' \rightarrow \alpha'$ transformation occurs near the center of each grain. The reason for appearing two types of isothermal transformation sequence in the sensitized SUS304 stainless steel is due to the difference in concentration by sensitization heat-treatment.

In chapter 5, we have investigated the effect of magnetic field on C-curve of successive $\gamma \rightarrow \varepsilon' \rightarrow \alpha'$ martensitic transformation in a solution-treated SUS304L stainless steel in order to clarify kinetics of the successive martensitic transformation, and we found that nose temperatures of C-curves do not depend on magnetic field strength (0.8, 4.0 and 5.6 MA/m), it is located at about 103 K for all the magnetic fields examined. This is due to the fact that $\gamma \rightarrow \varepsilon'$ martensitic transformation, having no concern with magnetic field, proceeds isothermally

while $\varepsilon' \rightarrow \alpha'$ martensitic transformation, influenced by magnetic field, proceeds athermally. C-curves shift to the side for a short time with increasing the strength of magnetic field because the magnetic energy difference between the ε'- and α'-phases provides a part of driving force, which is necessary for the $\varepsilon' \rightarrow \alpha'$ martensitic transformation.

The knowledge of martensitic transformation behavior obtained in the present study will be variable for using austenitic stainless steels under extreme environments.

Appendix

Kinetics of martensitic transformation

Martensitic transformations are usually classified into two groups from the kinetics of the transformation: athermal and isothermal ones. Concerning the kinetics of martensitic transformation, Kakeshita *et al.* have found that the originally isothermal kinetics of martensitic transformation in Fe-Ni-Mn based alloy changed to an athermal one under pulsed magnetic field higher than a critical one, which corresponds to the minimum strength of magnetic field to induce martensitic transformation at a given temperature, and they have also performed a systematic study on the incubation time in Fe-Ni-Mn alloys under magnetic field. They have explained their experimental results by introducing a new phenomenological theory. This theory is based on the probability related to the nucleation barrier. Moreover, it is predicted that the athermal martensitic transformation can be explained in the same kinetics as the isothermal martensitic transformation. Details of this theory are described below.

The new phenomenological theory gives a unified explanation for both the isothermal and athermal kinetics of martensitic transformation in such a way that the former transformation gives a C-curve but the latter transformation does not in their *TTT* diagram. The central idea

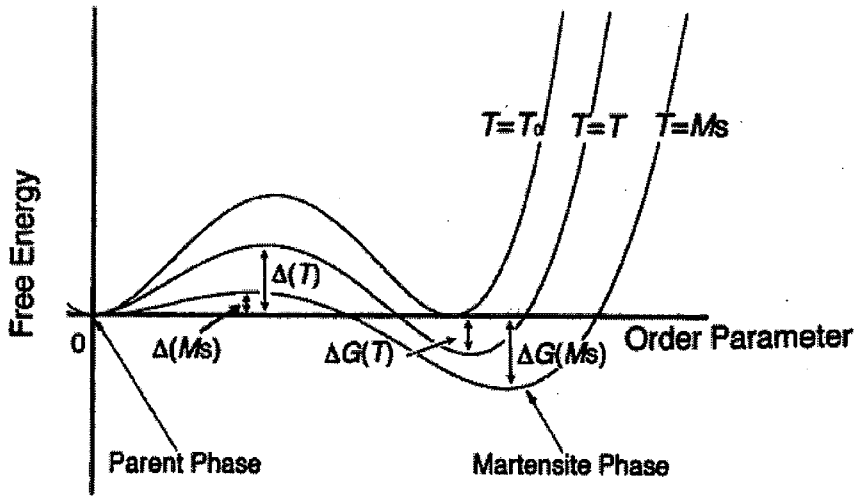

Fig. A-1. Schematic plot of the Gibbs chemical free energy as a function of the order parameter. (after Kakeshita *et al.* [1])

of this phenomenological theory is that martensitic transformation is assumed to occur by a thermally activated process, or a probability process, which will be described schematically using Fig. A-1. This figure shows the free energy as a function of order parameter (strain is usually taken as the order parameter of the martensitic transformation) for a system exhibiting a first order phase transition. It should be noted that the martensitic transformation does not occur at the equilibrium temperature, T_0, but at M_s which is below T_0 and a potential barrier (indicated by $\Delta(T)$ at a temperature, T) exists between the parent and the martensitic states. The existence of such a barrier is well known for a first-order phase transition and in this case the barrier may be related to the interfacial energy and the strain energy needed to start the transformation. They assume that the martensitic transformation macroscopically occurs when some particles (atoms, electrons) climb the potential barrier by thermal activation processes. This process naturally gives the time-dependent nature of the martensitic transformation in the following way; when the transition probability of particles over the potential barrier is high, a martensitic transformation occurs with a short incubation time. Therefore, the incubation time will be evaluated by the inverse of the transition probability. Based on the assumptions mentioned above, the meaning of the M_s temperature and the difference in the process between the athermal and isothermal martensitic transformations can be explained. That is, the transition probability of particles over the potential barrier is extremely high at the M_s temperature compared with any temperature higher than M_s. This is the meaning of the M_s temperature at which the martensitic transformation occurs instantaneously. The difference in process between athermal and isothermal transformations is whether a specific temperature exists where the transition probability becomes extremely high; such a temperature (M_s) exists for an athermal martensitic transformation and not for an isothermal martensitic transformation. Considering the above factors, they constructed a phenomenological theory, making the following three assumptions: (1) particles (atoms, electrons) must acquire a certain critical energy (a potential barrier mentioned above), Δ, before they can change the state from austenite to martensite. The potential barrier is expressed as $\Delta(T) = \Delta G(M_s) - \Delta G(T)$, where $\Delta G(M_s)$ and $\Delta G(T)$ represent the difference in Gibbs chemical free energies between the parent and

martensitic state at M_s and T, respectively; (2) the transition probability (P_e) from the austenitic state to the martensitic state is proportional to the Boltzmann factor and is expressed as

$$P_e = P_0 \cdot \exp(-\Delta / k_B T) \qquad \text{(A-1)}$$

where k_B is the Boltzmann constant and P_0 is a constant related to the cooperative movement of atoms which is a characteristic feature of martensitic transformations; (3) in the case of $\Delta \neq 0$, martensitic transformation does not start even if one particle is excited, but it does so when some critical number of particles, n^*, among the excited particles, m, form a cluster in the austenite. Based on these assumptions, the probability (P) of the occurrence of martensitic transformation has been derived as,

$$P = \sum_{m(\geq n \geq n^*)}^{N} \sum_{n(n \geq n^*)}^{m} f(N, M, n, n^*)(Pe)^m (1 - Pe)^{N-m} \qquad \text{(A-2)}$$

where N and n^* represent the total number of particles and a minimum number of particles in the cluster which is required to start a martensitic transformation, respectively, and m and n the number of excited particles and $f(N, m, n, n^*)$ the possible number of clusters consisting of n particles within m excited particles. If they assume that the well-known ergodic hypothesis holds in the present analysis, then the incubation time for a martensitic transformation to start can be evaluated by the inverse of P, P^{-1}. More details of the theory have been reported elsewhere[1-2].

Reference

[1] T. Kakeshita, T. Saburi and K. Shimizu, *Marls. Sci. and Eng. A* **273-275** (1999) 21

[2] T. Kakeshita, T. Yamamoto, K. Shimizu, K. Sugiyama and S. Endo, *Trans. JIM* **36** (1995) 1018

Publications related to this thesis

1. Jae-hwa Lee, Takashi Fukuda, Tomoyuki Kakeshita and Koichi Kindo

   Effects of Magnetic Field and Deformation on Isothermal Martensitic Transformation in SUS304 and SUS304L Steels

   Materials Transactions, **48** (2007) 2833-2839

2. Jae-hwa Lee, Takashi Fukuda and Tomoyuki Kakeshita

   Effect of Magnetic Field on Isothermal Martensitic Transformation in SUS304L Stainless Steel

   Materials Science Forum, **561-565** (2007) 2333-2336

3. Jae-hwa Lee, Takashi Fukuda and Tomoyuki Kakeshita

   Time-Temperature-Transformation Diagram of Successive $\gamma \rightarrow \varepsilon' \rightarrow \alpha'$ Martensitic Transformation in SUS304L Stainless Steel

   Materials Transactions, **49** (2008) 1937-1940

4. Jae-hwa Lee, Takashi Fukuda and Tomoyuki Kakeshita

   Isothermal Martensitic Transformation in Sensitized SUS304 Austenitic Stainless Steel at Cryogenic Temperature

   Materials Transactions, in press

5. Jae-hwa Lee, Takashi Fukuda and Tomoyuki Kakeshita

   Effect of Magnetic Field on *TTT* Diagram of Successive $\gamma \rightarrow \varepsilon' \rightarrow \alpha'$ Martensitic Transformation in SUS304L Stainless Steel

   Journal of Physics: Conference Series, in press

6. Jae-hwa Lee, Takashi Fukuda and Tomoyuki Kakeshita

Effect of Temperature and Magnetic Field on Stability of Austenitic Phase in SUS304L Stainless Steel

Submitted to TMS

7. Jae-hwa Lee, Takashi Fukuda and Tomoyuki Kakeshita

Martensitic Transformation Behavior in Sensitized SUS304 Austenitic Stainless Steel during Isothermal Holding at Low Temperature

Submitted to Journal of Physics: Conference Series

Other Publication

1. Takashi Fukuda, Motohiro Yuge, Jae-hwa Lee, Tomoyuki Terai and Tomoyuki Kakeshita

Effect of Magnetic Field on $\gamma \rightarrow \alpha$ Transformation Temperature in Fe-Co Alloys

ISIJ International, **46** (2006) 1267-1270

Presentation at international conferences

1. Jae-hwa Lee, Takashi Fukuda, Tomoyuki Kakeshita and Koichi Kindo

   'Effects of Magnetic Field and Deformation on Isothermal Martensitic Transformation in SUS304 and SUS304L Steels'

   PRICM-6, Jeju, Korea, November, 2007

2. Jae-hwa Lee, Takashi Fukuda and Tomoyuki Kakeshita

   'Effect of Magnetic Field on Isothermal Martensitic Transformation in an Fe-Ni-Mn alloy'

   ICMS2007, Hiroshima, Japan, November, 2007

3. Jae-hwa Lee, Takashi Fukuda and Tomoyuki Kakeshita

   'Effect of Magnetic Field on *TTT* Diagram of Successive $\gamma \rightarrow \varepsilon' \rightarrow \alpha'$ Martensitic Transformation in SUS304L Stainless Steel'

   MAP3, Tokyo, Japan, May, 2008

4. Jae-hwa Lee, Takashi Fukuda and Tomoyuki Kakeshita

   'Effect of Temperature and Magnetic Field on Stability of Austenitic Phase in SUS304L Stainless Steel'

   ICOMAT-08, New Maxico, USA, June, 2008

5. Jae-hwa Lee, Takashi Fukuda and Tomoyuki Kakeshita

   'Martensitic Transformation Behavior in Sensitized SUS304 Austenitic Stainless Steel during Isothermal Holding at Low Temperature'

   ASFMD2008, Osaka, Japan, November, 2008

Acknowledgments

This work has been carried out under the guidance of *Prof. Tomoyuki Kakeshita* at Division of material and manufacturing science, Osaka University. The author would like to express his grateful gratitude to *Prof. Tomoyuki Kakeshita* for his kind guidance, helpful suggestions and invaluable encouragements throughout this work. The author would like to thank *Prof. Hirotaro Mori* and *Prof. Hideki Araki* at Division of material and manufacturing science, Osaka University for reviewing this thesis and their helpful advice.

The author is very grateful to *Prof. Takashi Fukuda* and *Prof. Tomoyuki Terai* at *Prof. Kakeshita's* Group for their helpful suggestion, discussion and guidance throughout this work.

The author wishes to make grateful acknowledge to *Prof. Tae-Hyun Nam* at Gyeongsang national university for his hearty encouragement and helps. The author also thanks the members in the *Prof. Nam's* Group for their friendships, encouragement and helps.

The author would like to thank past and present students in the *Prof. Kakeshita's* Group, *Dr. Jae-hoon Kim*, *Dr. Mi-Seon Choi*, *Dr. Tatsuaki Sakamoto*, *Mr. Motoyoshi Yasui*, *Mr. Hiroaki Kushida*, *Ms. Sahar Farjami* and *Mr. Mitsuharu Todai* for their friendships and helps.

The author is very grateful to *Dr. Duk-ki Lee*, *Dr. Tae-mok kwon*, *Dr. Yong-jun choi*, *Mr. Tae-bum Kim*, *Mr. young-dong Jung* and *Mr. Min-hyo shin* for their friendships, encouragement and helps.

This study was supported by "Priority Assistance for the Formation of Worldwide Renowned Centers of Research-The 21st Century COE Program (Project: Center of Excellence

for Advanced Structural and Functional Materials Design)" and "Priority Assistance for the Formation of Worldwide Renowned Centers of Research-The Global COE Program (Project: Center of Excellence for Advanced Structural and Functional Materials Design)" from the Ministry of Education, Culture, Sports, Science and Technology (MEXT), Japan.

Finally, the author wishes to express the deep appreciation to the author's parents, my elder brother and his wife for their encouragements, understanding and support.

Jae-Hwa Lee

December 2008